

Inhibition of Stromelysin-1 (MMP-3) by P₁'-Biphenylethyl Carboxyalkyl Dipeptides

Craig K. Esser,* Robert L. Bugianesi, Charles G. Caldwell, Kevin T. Chapman, Philippe L. Durette, Narindar N. Girotra, Ihor E. Kopka, Thomas J. Lanza, Dorothy A. Levorse, Malcolm MacCoss, Karen A. Owens, Mitree M. Ponpipom, Joseph P. Simeone, Richard K. Harrison,† Lisa Niedzwiecki,† Joseph W. Becker,‡ Alice I. Marcy,‡ Melinda G. Axel,‡ Amy J. Christen,‡ Joseph McDonnell,‡ Vernon L. Moore,‡ Julie M. Olszewski,‡ Cheryl Saphos,‡ Denise M. Visco,‡ Frank Shen,|| Adria Colletti,§ Philip A. Krieter,§ and William K. Hagmann

Departments of Medicinal Chemistry, Enzymology, Pharmacology, Biophysical Chemistry, Biometrics, and Drug Metabolism, Merck Research Laboratories, P.O. Box 2000, Rahway, New Jersey 07065-0900

Received June 28, 1996[⊗]

Carboxyalkyl peptides containing a biphenylethyl group at the P₁' position were found to be potent inhibitors of stromelysin-1 (MMP-3) and gelatinase A (MMP-2), in the range of 10–50 nM, but poor inhibitors of collagenase (MMP-1). Combination of a biphenylethyl moiety at P₁', a *tert*-butyl group at P₂', and a methyl group at P₃' produced orally bioavailable inhibitors as measured by an *in vivo* model of MMP-3 degradation of radiolabeled transferrin in the mouse pleural cavity. The X-ray structure of a complex of a P₁'-biphenyl inhibitor and the catalytic domain of MMP-3 is described. Inhibitors that contained halogenated biphenylethyl residues at P₁' proved to be superior in terms of enzyme potency and oral activity with 2(*R*)-[2-(4'-fluoro-4-biphenyl)ethyl]-4(*S*)-*n*-butyl-1,5-pentanedioic acid 1-(α (*S*)-*tert*-butylglycine methylamide) amide (L-758,354, **26**) having a *K*_i of 10 nM against MMP-3 and an ED₅₀ of 11 mg/kg po in the mouse pleural cavity assay. This compound was evaluated in acute (MMP-3 and IL-1 β injection in the rabbit) and chronic (rat adjuvant-induced arthritis and mouse collagen-induced arthritis) models of cartilage destruction but showed activity only in the MMP-3 injection model (ED₅₀ = 6 mg/kg iv).

Introduction

The matrix metalloproteinases are a family of zinc-containing, calcium-dependent endopeptidases that are capable of hydrolyzing the extracellular matrix of connective tissues and basement membranes.^{1–7} Although their roles in the normal and pathological turnover of these tissues are not completely understood,⁸ the elevated levels of these enzymes, particularly stromelysin-1 (MMP-3) and collagenase-1 (MMP-1), found in the synovium and cartilage of osteoarthritis and rheumatoid arthritis patients have suggested a role for these enzymes in these disease processes.^{9–15} Gelatinase A (MMP-2) is particularly proficient at degrading basement membranes and is thought to play a role in tumor metastasis.¹⁶ Therefore, there has been substantial interest in developing MMP inhibitors for a variety of therapeutic indications.^{17–27}

We have focused on the discovery of potent, selective inhibitors of MMP-3.^{28–30} By structure–activity relationship (SAR) studies and structural analysis, we and others have discovered that the S₁' binding pockets of MMP-3 and MMP-1 differ considerably. MMP-3 has a deep, hydrophobic S₁' hole that extends through the enzyme, whereas the S₁' pocket of MMP-1 is much shallower.^{29,31–37} We also discovered that substituted carboxyalkyl dipeptides have significant oral activity in an animal model of MMP-3-induced macromolecular degradation.³⁰ Herein, we report the discovery of P₁'-

biphenylethyl-containing carboxylate inhibitors of MMP-3 with enhanced enzyme potency and oral activity and their evaluation in animal models of cartilage degradation.

Chemistry

A synthesis of the carboxyalkyl peptide inhibitors is shown in Scheme 1. Starting from commercially available (4-iodophenyl)butyric acid (**1**), the mixed anhydride, obtained with trimethylacetyl chloride, was reacted with the lithium anion of (*S*)-4-benzyl-2-oxazolidinone to afford **2**. Following procedures described by Evans,³⁸ enantioselective Michael addition of the titanium enolate of the chiral oxazolidinone **2** to *tert*-butyl acrylate provided **3** having the carboxylate functionality with a suitable protecting group. Hydrolysis of the chiral auxiliary with lithium hydroxide and hydrogen peroxide yielded the carboxylic acid **4**. Alkylation of the lithium dianion of **4** with iodobutane produced **5** as a mixture of diastereomers (~3:1) in favor of the desired 4*S*,2*R* isomer. Separation of the desired diastereomer of acid **5** was not efficient, so the mixture was converted to its (trimethylsilyl)ethyl ester using (trimethylsilyl)ethanol and 1-[3-(dimethylamino)propyl]-3-ethylcarbodiimide hydrochloride (EDC) and then purified by silica gel chromatography to separate the diester **6** as the pure 4*S*,2*R* diastereomer. This diester contains the P₁ and P₁' portion of our inhibitors along with the iodo functionality at the 4-position of the phenyl ring and served as a key intermediate in the modification of the P₁' portion of our inhibitors.

The 4-iodophenethyl intermediate was modified by various carbon–carbon bond-forming methodologies reported in the literature. Palladium-catalyzed boronic acid coupling methodology described by Suzuki and

* To whom correspondence and reprint requests should be sent.

† Department of Enzymology.

‡ Department of Pharmacology.

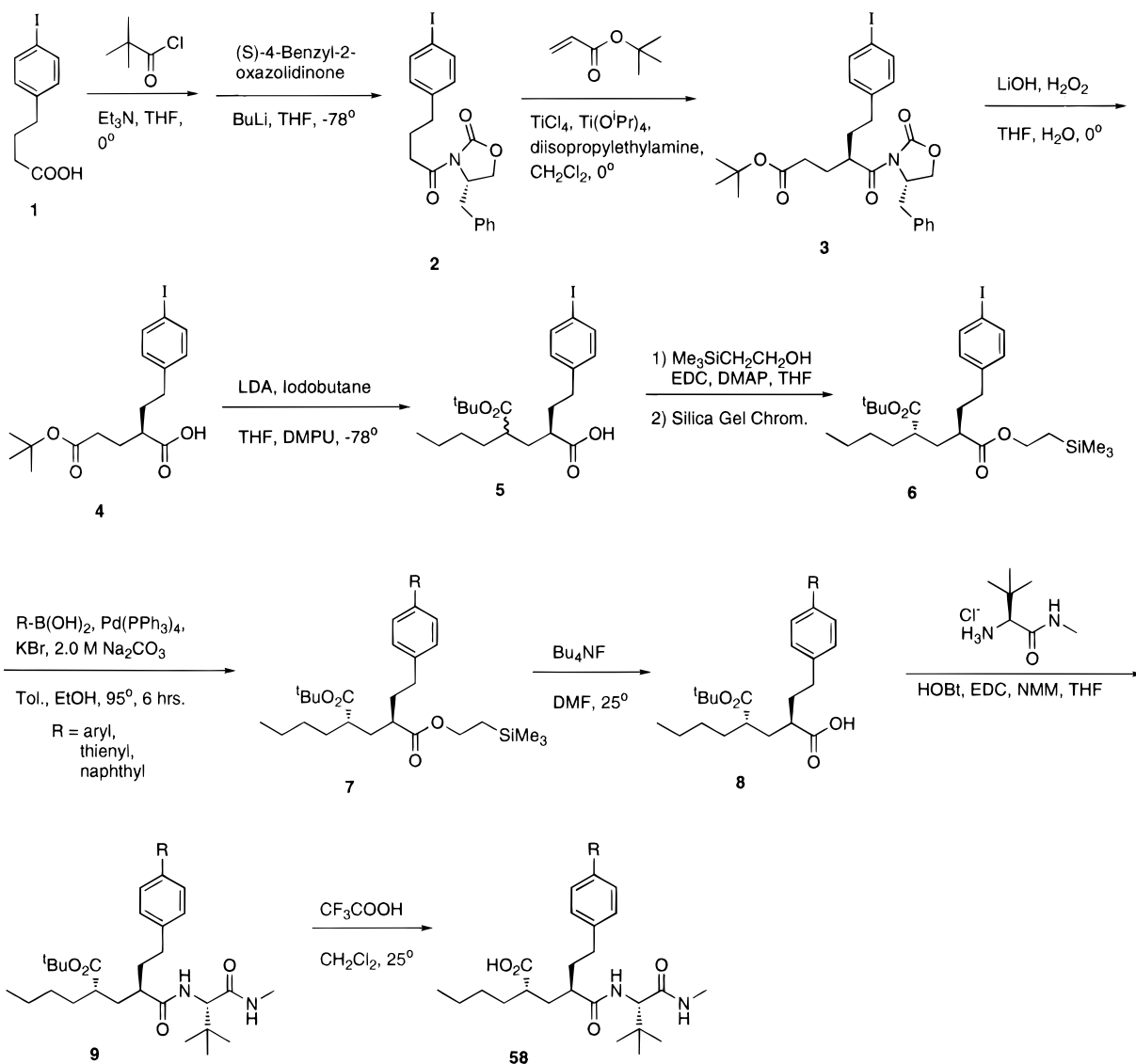
§ Department of Drug Metabolism.

¶ Department of Biophysical Chemistry.

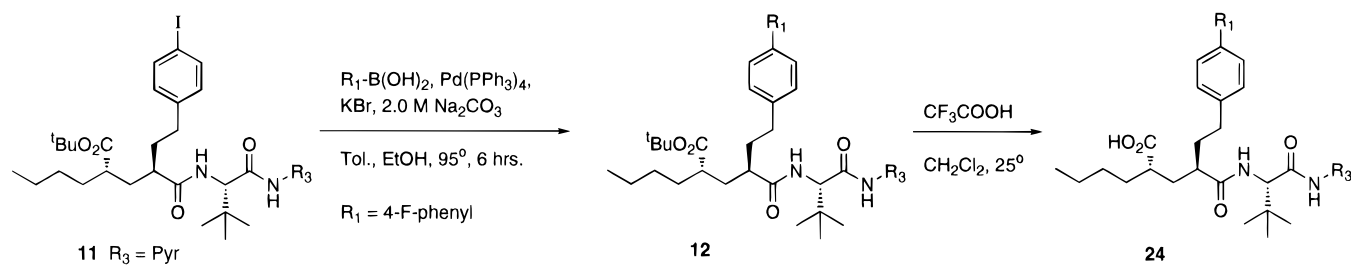
|| Department of Biometrics.

⊗ Abstract published in *Advance ACS Abstracts*, February 15, 1997.

Scheme 1



Scheme 2



others^{39–43} introduced the biphenyl moiety into our inhibitors as illustrated in Scheme 1. Reacting intermediate **6** with substituted arylboronic acids in the presence of palladium(0) and a base generated biphenyls of the general structure **7** in satisfactory yields (50–80%). The TMS-ethyl ester in **7** was removed with tetrabutylammonium fluoride, and the resulting acid **8** was coupled with (*S*)-*tert*-butylglycine methylamide hydrochloride in the presence of *N*-methylmorpholine (NMM), *N*-hydroxybenzotriazole (HOBt), and EDC. Cleavage of the *tert*-butyl ester with trifluoroacetic acid (TFA) afforded the carboxyalkyl peptides **58** as listed in Tables 1 and 2.

Alternatively, as shown in Scheme 2, biphenyl forma-

tion using Suzuki conditions was also performed later in the synthetic scheme on the larger dipeptide **11** followed by deprotection with TFA to yield the desired carboxylate inhibitors. However, the Suzuki coupling proceeded in better yield on the diester **6** compared to the dipeptide **11** (75% vs 55% yields).

A less convergent but more directed method for modifying the P₁' portion of our inhibitors is shown in Scheme 3. The desired P₁' moiety (**13**, for example) was acylated with succinic anhydride under Friedel–Crafts conditions to yield 4-keto-4-biphenylbutyric acid **14**. The ketone was then reduced with hydrogen in the presence of Pearlman's catalyst to afford the substituted

Scheme 5

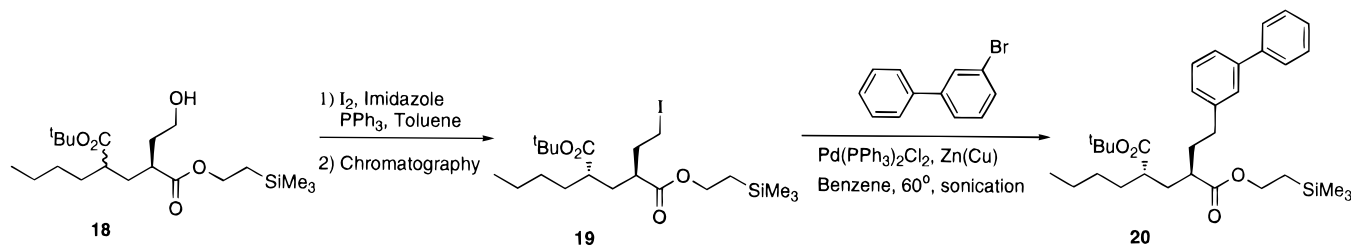


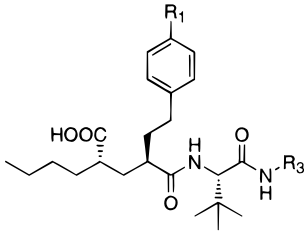
Table 1. Inhibition of Human MMP-3 and MMP-2 by Carboxyalkyl Peptides

compd no. ^c	R ₁ (P ₁)	R ₃ (P ₃)	K _i , nM ^a		PLCAV ^b % inh @ 60 mpk, po
			MMP-3	MMP-2	
24	4-F	4-pyridyl	2.0 ± 0.2	25 ± 2	72 ± 10
25	4-F	Ph	4 ± 1	150 ± 10	61 ± 4
26	4-F	CH ₃	10 ± 1	17 ± 1	93 ± 2
27	3-NH ₂	Ph	27 ± 3	280 ± 30	4 ± 6
28	4-CF ₃	CH ₃	37 ± 3	39 ± 4	78 ± 7
29	3-CF ₃	CH ₃	1100 ± 100	3600 ± 500	17 ± 9
30	4-Cl	CH ₃	13 ± 2	25 ± 2	84 ± 3
31	3,5-diCl	CH ₃	1500 ± 100	1600 ± 100	0
32	2,4-diCl	CH ₃	12 ± 1	100 ± 10	62 ± 3
33	4-Ph	CH ₃	39 ± 4	84 ± 9	22 ± 12
34	3-Cl,4-F	CH ₃	19 ± 2	80 ± 8	61 ± 10
35	4-Br	CH ₃	11 ± 1	17 ± 2	90 ± 2
36	3-F	CH ₃	21 ± 1	48 ± 5	72 ± 6
37	2-F	CH ₃	11 ± 1	61 ± 7	87 ± 2
38	4-CN	CH ₃	9 ± 1	14 ± 2	80 ± 17
39	4-SCH ₃	CH ₃	5 ± 1	13 ± 1	84 ± 5
40	4-SO ₂ CH ₃	CH ₃	21 ± 1	19 ± 2	37 ± 11
41	4-SOCH ₃	CH ₃	52 ± 5	30 ± 2	21 ± 11
42	2,6-diCH ₃	CH ₃	1200 ± 100	1300 ± 100	ND ^e
43	4-CHO	CH ₃	15 ± 1	16 ± 1	7 ± 12
44	4-(2-imidazolyl)	CH ₃	25 ± 2	94 ± 8	17 ± 7
45	4-COOH	CH ₃	690 ± 30	580 ± 50	13 ± 5
46	4-(5-tetrazolyl)	CH ₃	350 ± 40	1800 ± 100	ND
47	4-OCH ₃	CH ₃	13 ± 1	21 ± 2	90 ± 3
48	2-SO ₂ NH- <i>t</i> -C ₄ H ₉	CH ₃	10% @ 10 ^d	17% @ 10 ^d	ND
49	2-SO ₂ NH ₂	CH ₃	9400 ± 1000	0% @ 10	ND
50	4-CO ₂ CH ₃	CH ₃	31 ± 3	32 ± 2	ND
51	4-CONH ₂	CH ₃	24 ± 1	38 ± 4	3 ± 4
52	4-CONHCH ₃	CH ₃	49 ± 4	34 ± 4	7 ± 9
53	4-CON(CH ₃) ₂	CH ₃	40 ± 3	50 ± 4	40 ± 20

^a All compounds listed were evaluated as inhibitors of human stromelysin-1 (MMP-3) and gelatinase A (MMP-2) by the methods previously described (±SE).²⁸ ^b Percent inhibition (±SE) of MMP-3-mediated degradation of radiolabeled transferrin in the mouse pleural cavity (PLCAV) after 60 mpk oral dose of inhibitor. ^c Compounds were purified to homogeneity and satisfactory elemental analyses or exact masses from high-resolution mass spectrometry were obtained (±0.4% of calculated values). ^d Indicates percent inhibition at 10 μM. ^e Not determined.

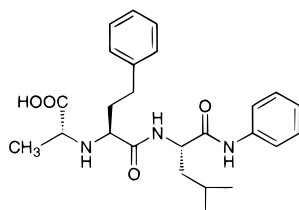
previously described,²⁸ and the results are reported in Tables 1 and 2. It should be noted that, in addition to K_i determinations against MMP-3 and MMP-2, several compounds (**24–26**, **33**, **65**, **66**) were evaluated as inhibitors of recombinant human fibroblast MMP-1. Each of these compounds proved to be an extremely weak inhibitor of MMP-1 (K_i > 10 μM). Generally, structures containing the biphenyl moiety at P₁' were poor MMP-1 inhibitors, so evaluation of these compounds against MMP-1 was not continued.

The methodology used to evaluate inhibition of MMP-3-mediated degradation of a macromolecular substrate by these compounds *in vivo* is similar to that described for the rat pleural cavity.^{30,55} The inhibition of the degradation of radiolabeled transferrin by human MMP-3 in the mouse pleural cavity was measured. Mice were pre-dosed orally with compound, after which a solution of [³H]transferrin was injected intrapleurally. This was followed immediately by the injection of trypsin-activated human MMP-3. After 30 min, the animals

Table 2. Inhibition of Human MMP-3 and MMP-2 by Carboxyalkyl Peptides


compd no. ^c	R ₁ (P ₁)	R ₃ (P ₃)	K _i , nM ^a		PLCAV ^b % inh @ 60 mpk, po
			MMP-3	MMP-2	
54	<i>n</i> -C ₃ H ₇	4-pyridyl	11 ± 1	22 ± 2	89 ± 4
55	CH ₂ Ph	Ph	1400 ± 200	16% @ 10 ^d	15 ± 9
56	<i>n</i> -C ₃ H ₇	CH ₃	140 ± 20	47 ± 3	ND ^e
57	3-Ph	CH ₃	1500 ± 100	2400 ± 200	ND
58	3-thienyl	CH ₃	15 ± 1	21 ± 1	70 ± 9
59	1-naphthyl	CH ₃	2000 ± 200	6900 ± 700	19 ± 4
60	CH=CHPh	CH ₃	65 ± 6	760 ± 80	ND
61	CH ₂ CH ₂ Ph	CH ₃	49 ± 5	380 ± 30	ND
62	2-indolyl	CH ₃	12 ± 1	49 ± 4	34 ± 20
63	OPh	CH ₃	200 ± 10	3000 ± 300	39 ± 11
64	2-naphthyl	CH ₃	120 ± 10	800 ± 100	65 ± 8
65	4-cycloheptyl	CH ₃	95 ± 10	1900 ± 200	48 ± 10
66	H	CH ₃	3800 ± 200	1500 ± 100	ND
67	2-THF	CH ₃	1400 ± 100	810 ± 80	ND
68	OCH ₂ Ph	CH ₃	74 ± 6	210 ± 20	ND

^a All compounds listed were evaluated as inhibitors of human stromelysin-1 (MMP-3) and gelatinase A (MMP-2) by the methods previously described (\pm SE).²⁸ ^b Percent inhibition (\pm SE) of MMP-3-mediated degradation of radiolabeled transferrin in the mouse pleural cavity (PLCAV) after 60 mpk oral dose of inhibitor. ^c Compounds were purified to homogeneity and satisfactory elemental analyses or exact masses from high-resolution mass spectrometry were obtained (\pm 0.4% of calculated values). ^d Indicates percent inhibition at 10 μ M. ^e Not determined.



L-696,418

MMP-3 K_i = 310 nMPLCAV ED₅₀ ≥ 100 mg/kg po**Figure 1.** Structure of an *N*-carboxyalkyl inhibitor of MMP-3-mediated cartilage degradation in the rabbit.^{56–59}

were sacrificed, and the pleural cavity was lavaged. After centrifugation, the amount of trichloroacetic acid-soluble and -precipitable counts were measured and compared to controls to give a percent inhibition of MMP-3 degradation of the transferrin. Results are reported in Tables 1 and 2 under the heading PLCAV.

Previously, we had shown that an *N*-carboxyalkyl dipeptide MMP inhibitor (L-696,418) was capable of inhibiting proteoglycan release from cartilage in a rabbit knee joint treated intraarticularly with human MMP-3 (Figure 1).^{56,57} That same inhibitor was also efficacious (~50%) in limiting the amount of proteoglycan release from a rabbit knee joint treated intraarticularly with human IL-1 β .^{58,59} These two injection models represent acute cartilage degradation initiated by exogenous enzyme or cytokine. L-696,418 did not have sufficient potency, selectivity, or duration of action to be considered for more chronic models of cartilage degradation.

On the basis of a more satisfactory pharmacokinetic profile (Table 3), compound **26** (L-758,354) was chosen to be evaluated in several models of cartilage destruction

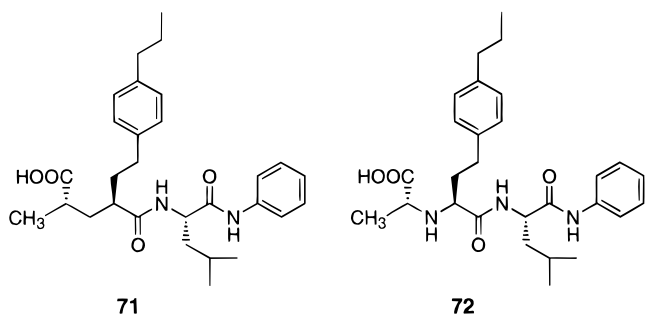
Table 3. Pharmacokinetic Properties of **26**^a

	mouse ^b	rat ^b	rabbit ^c
plasma <i>t</i> _{1/2} (h)	2.7	4.4	0.9
clearance (mL/min/kg)	1.1	1.3	7.6
<i>V</i> _{dss} (L/kg)	0.20	0.32	0.20
oral bioavailability ^d	78%	60%	ND ^e

^a Compound levels were determined by RP-HPLC relative to a standard curve (see the Experimental Section). ^b 20 mg/kg iv. ^c 12 mg/kg iv. ^d 20 mg/kg po. ^e ND = not determined.

and inflammatory arthritis. Inhibitor **26** was administered to rabbits intravenously 15 min prior to the injection of activated human recombinant fibroblast MMP-3 into the stifle joint according to the published procedures.^{56,57} The contralateral joint served as the control knee. In the IL-1 β injection model,⁵⁸ compound **26** was administered (12 mg/kg iv) six times every 2 h from the time of the IL-1 β injection. In both models, synovial lavage fluid was analyzed for released proteoglycan by an alcian blue assay.^{56,57}

In the rat adjuvant-induced arthritis (AIA) model,^{60,61} inhibitor **26** was administered at 50 mg/kg po b.i.d. throughout the 21 days of the experiment. Indomethacin (1 mg/kg po b.i.d.) served as the positive control. Body weights, foot volumes, and thymus and spleen weights were used to measure efficacy. In the mouse collagen-induced arthritis (CIA) model,⁶² **26** was also administered at 50 mg/kg po b.i.d. throughout the course of the experiment. Indomethacin (1 mg/kg po s.i.d.), dexamethasone (1 mg/kg po s.i.d.), and cyclophosphamide (5 mg/kg po s.i.d.) served as positive controls. Severity scores and percent incidence were used to evaluate efficacy. Levels of total drug concentration in plasma were determined at the time of euthanasia.



MMP-3 K_i = 68 nM
PLCAV ED_{50} = 32 mg/kg po

MMP-3 K_i = 18 nM
PLCAV ED_{50} = 65 mg/kg po

Figure 2. Comparison of *C*- vs *N*-carboxyalkyl peptide inhibitors of MMP-3 in the mouse pleural cavity assay.³⁰

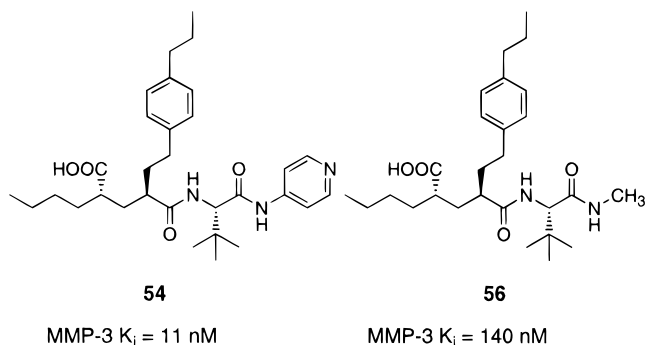
Results and Discussion

The starting point for this study was the carboxyalkyl dipeptide inhibitor 2(*R*)-[2-(4-*n*-propylphenyl)ethyl]-4(*S*)-methylpentanedioic acid 1-((*S*)-leucine phenylamide) amide (**71**), MMP-3 K_i = 68 nM (Figure 2).³⁰ More importantly, this compound showed a significant increase in oral activity compared to its *N*-carboxyalkyl analog **72** as measured in the pleural cavity assay. Figure 2 reports these results as the dose in mg/kg required to inhibit 50% of the human MMP-3 degradation of transferrin in the mouse pleural cavity compared to the control group (ED_{50}). This result, combined with the increased potency and selectivity for MMP-3 inhibition found for the 4-propylphenethyl group at the P_1' position,⁶⁴ suggested that additional gains in potency and/or oral activity might be achievable by further modification of the P_1' -phenethyl side chain in this class of carboxyalkyl peptides.

In addition to modifying the P_1' position, we sought to optimize other subsites of this class to achieve the desired combination of potency, selectivity, and pharmacokinetic properties for an MMP-3 inhibitor. An increase in potency has been observed with cyclic imido^{30,65–70} and lipophilic^{66,68} groups at the P_1 position. We found that the *n*-butyl group provided for enhanced potency versus MMP-3 as well as improved oral activity,⁶⁹ and thus, it became the substituent of choice for the P_1 position in this study. The *tert*-butyl group at P_2' had been found to improve plasma stability and oral absorption in a series of MMP-1 inhibitors.^{23,25,70} The *tert*-butyl group sterically hinders hydrolysis of the P_2' – P_3' amide bond and was also held constant in this study.

Inhibition of MMP-3 had been shown to be enhanced by a P_3' -aryl group.^{28,71,72} However, metabolic cleavage of the P_2' – P_3' amide bond would produce an aromatic amine as a potentially toxic byproduct (e.g., aniline). Many groups have incorporated a methyl group at P_3' in their inhibitor designs,^{65,66,68,70,73,74} but this substitution led to a decrease in activity against MMP-3 in our earlier designs.⁷⁵ For example, compound **54** has a K_i = 11 nM against MMP-3, but when the 4-pyridyl group is replaced by methyl, the MMP-3 activity diminishes to a K_i of 140 nM for compound **56** (Figure 3).

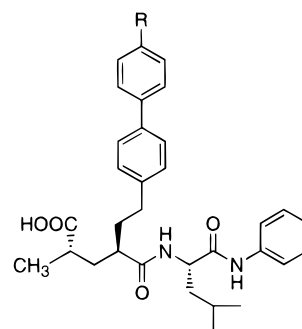
In compounds related to **54** where the P_2' – P_3' amide bond was stabilized by a P_2' -*tert*-butyl group, it was found that the *n*-propyl group was metabolized by isolated rat liver microsomes and also *in vivo* in rats.⁷⁶ Several metabolites were isolated and determined to be oxidized derivatives of the *n*-propyl group. In an effort



MMP-3 K_i = 11 nM

MMP-3 K_i = 140 nM

Figure 3. Comparison of P_3' -aryl vs -methyl substitution on MMP-3 activity of P_1' -4-*n*-propylphenethyl inhibitors.



R = H; MMP-3 K_i = 82 nM
R = F; MMP-3 K_i = 38 nM

Figure 4. Effect of 4'-fluoro substitution in the P_1' -biphenylethyl group on MMP-3 activity.

to both block this metabolism and possibly enhance potency, P_1' -4-biphenyl analogs were prepared. Our major focus was on substituted biphenyl derivatives, as the unsubstituted parent in a related series was a somewhat less active MMP-3 inhibitor (Figure 4). Additionally, it was assumed that substituents, particularly electron-withdrawing ones, would decrease potential oxidative metabolism of the biaryl system, and this protection may also extend to the connecting benzylic position. Thus, compounds **24**–**26** provide the basis for comparison with the inhibitors described herein.

The combination of biphenyl substitution at P_1' with methyl substitution at P_3' enhanced the oral activity of these inhibitors as measured in the mouse pleural cavity assay. Compound **26**, which combines a (4-fluorobiphenyl)ethyl side chain at P_1' and a methyl group at P_3' , shows almost a 3-fold improvement in oral activity in the pleural cavity assay compared to the corresponding analog containing a phenyl group at P_3' (**25**).

As seen in Table 1, halogen substitution on the second (or outer) phenyl ring is generally well tolerated by both MMP-3 and MMP-2 with a few exceptions. The poor activity of the 3',5'-dichloro analog **31** suggests a lack of steric symmetry in the P_1' site, whereas a 3'-chloro substituent in **34** is tolerated. Fluorine is acceptable in any position (**26**, **36**, **37**). The 4'-trifluoromethyl group in **28** is active but not at the 3'-position in **29**. Possibly, the high dipolar nature of this substituent imparts unfavorable interactions in this region.

The 4'-position will tolerate a wide variety of substitution. In particular, the terphenyl analog **33** (three phenyl rings in a linear arrangement) illustrates the nature of the S_1' pocket of these two enzymes. Structural studies have shown that the S_1' site in MMP-3 is

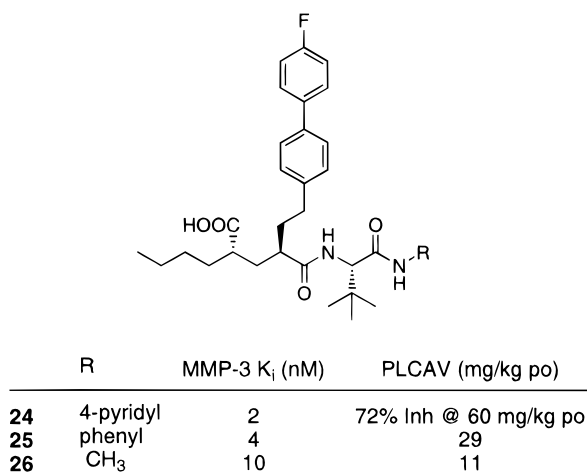


Figure 5. Comparison of P₃'-aryl vs -methyl substitution of P₁'-(4'-fluorobiphenyl)ethyl inhibitors on MMP-3 and mouse pleural cavity activities.

a hole that extends completely through the enzyme.^{33,34} Modeling studies with **33** show that the third phenyl ring extends out the other side of this hole. It is intriguing that the enzymes are able to accommodate such a large, rigid structure into their deep, albeit tight fitting, S₁' sites.

Compound **26** is highly protein bound (97.6% in rabbit plasma and 99.8% in the presence of human serum albumin).⁷⁶ As such, its bioavailability might be expected to be reduced, and thus, a more polar inhibitor was sought. It was found that polar or charged substituents at the P₂' or P₃' positions had little effect on protein binding or measured log *P* values and that the biphenylethyl group was the dominating feature in determining protein binding.

X-ray crystallographic studies of MMP-3 had shown that the S₁' pocket contains several carbonyl oxygen atoms that could serve as hydrogen bond acceptors,³⁴ but a more definitive structure of a P₁'-biphenyl inhibitor complexed to the catalytic site of MMP-3 was needed (Figure 6 and Supporting Information, Table 1). The overall structure of the SLN-247 (residues 83–247) complex with L-764,004 is quite similar to that of the SLN-255 (residues 83–255) complex with L-702,842 when the structures are aligned on all α -carbon atoms, the average deviation being only 0.38 Å (rms 0.48 Å), despite the differences in construct, inhibitor, and crystal lattice (Figure 7).^{33,34} The only α -carbon atoms that are separated by more than 1.0 Å in the aligned structures are at residues 190, 225, and 228, positions in apparently mobile regions as judged by their higher than normal temperature factors. The alkyl chain on the unprimed side of the inhibitor lies in an extension of the binding site groove, and the benzolactam lies in a shallow depression in the enzyme surface defined by Ala167 and the side chains of Tyr155, His166, and Tyr168. In addition, this group makes a lattice-specific stacking interaction with the side chain of Phe210 from another residue. The two rings are parallel to each other and approximately 3.8 Å apart.

In contrast with this general similarity, there are several significant differences in how the inhibitors interact with the enzyme. First, when the structures are aligned on the α -carbon atoms of the enzyme, there is a shift of the bound inhibitor toward the primed side of the binding site: the P₁' α -carbons are 0.85 Å apart;

P₂', 0.95 Å. As a consequence of this movement, there is a change in the hydrogen-bonding pattern (Supporting Information, Table 2). The shift in binding geometry correlates with changing the atom at the P₁'N position from a nitrogen in the L-702,842 complex to a carbon in the L-764,004 complex. A nitrogen atom in this position can form hydrogen bonds with Ala165O and Glu202O^{e2}, while a carbon atom must move away from these polar atoms. A consequence of this shift is the strengthening of the polar interaction between the P₂'N and Pro221O atoms in the complex with L-764,004: these atoms are 3.36 Å apart in this complex as compared with a separation of 3.82 Å in the complex with L-702,842. Another significant difference is the conformation of the P₁' side chain: in the complex with L-702,842, the P₁'-phenylethyl group adopts a *ttg*⁻ conformation, while the corresponding arrangement in the complex with L-764,004 is *g*⁺*tg*⁻ (Supporting Information, Table 3). Despite this difference, the comparable aromatic rings occupy roughly the same volume in the two complexes. The interactions of the first ring of the biphenyl moiety of L-764,004 with specific protein groups are similar to those seen in the complex with L-702,842: the ring is parallel with the side chain of His201, the carbonyl oxygen atoms of Leu218 and Tyr220 point toward the ring, and the side chain of Tyr223 is directed toward the center of the ring. The dihedral angle between the two rings is 49°, and the second ring interacts with both sides of the S₁' subsite, making van der Waals contacts with Ala217 and Leu218 on one side and with Leu191, Tyr223, His224, and Leu226 members of the flexible loops on the outside of the site.

As a result of modeling studies with this X-ray structure, polar (**40**, **41**, **43**, **48–53**) or charged (**44–46**) substituents on the biphenyl group were introduced in search of potential hydrogen-bonding interactions within the S₁' pocket that would reduce overall protein binding and possibly enhance potency. Unfortunately, these structures were less potent than the halogenated analogs. In addition, oral activity in the pleural cavity model was significantly reduced. For example, compound **51** had reasonably good activity against MMP-3 ($K_i = 24$ nM) but was inactive in the pleural cavity assay (3% inhibition at 60 mg/kg po).

Efforts to uncover a different scaffold that bound into the S₁' pocket of MMP-3 more efficiently than the P₁'-4-biphenylethyl side chain of **26** were also not successful. For example, **57** (3-biphenylethyl group at P₁') and **59** (1-naphthylphenethyl group at P₁') lost 2 orders of magnitude in potency against MMP-3, further supporting the observation that the S₁' pocket is deep but relatively narrow. Some of the compounds in Table 2 showed similar activity to **26** against MMP-3 *in vitro* but did not exhibit comparable oral activity in the pleural cavity assay. For example, compound **62** has a $K_i = 12$ nM but has low activity in the pleural cavity assay (34% inhibition at 60 mg/kg). Overall, a number of different hydrophobic scaffolds were explored that led to comparable potencies against MMP-3, but none exhibited any advantages over **26**.

Figure 8 summarizes the structural changes to compound **72** that were investigated and the resulting effects these changes had on the potency and pharmacokinetic properties of these inhibitors. Alkyl groups

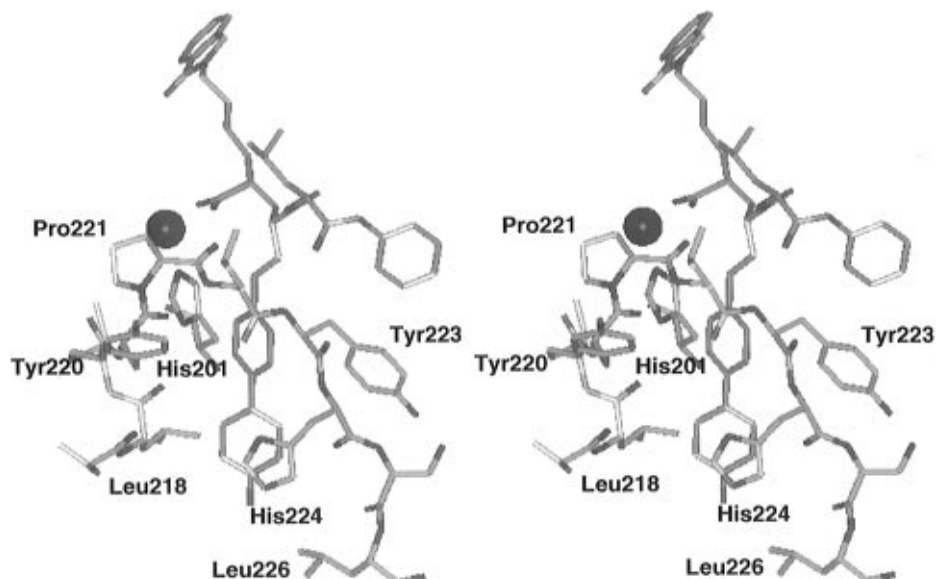


Figure 6. S_1' site. The inhibitor L-764,004 (see Figure 7) in gray carbon atoms is shown together with all groups of the catalytic core that surround the P_1' -(4'-fluoro-4-biphenyl)ethyl group (light green carbon atoms). The catalytic zinc is represented as a violet sphere, and the zinc ligand His201 is shown at the rear of the figure.

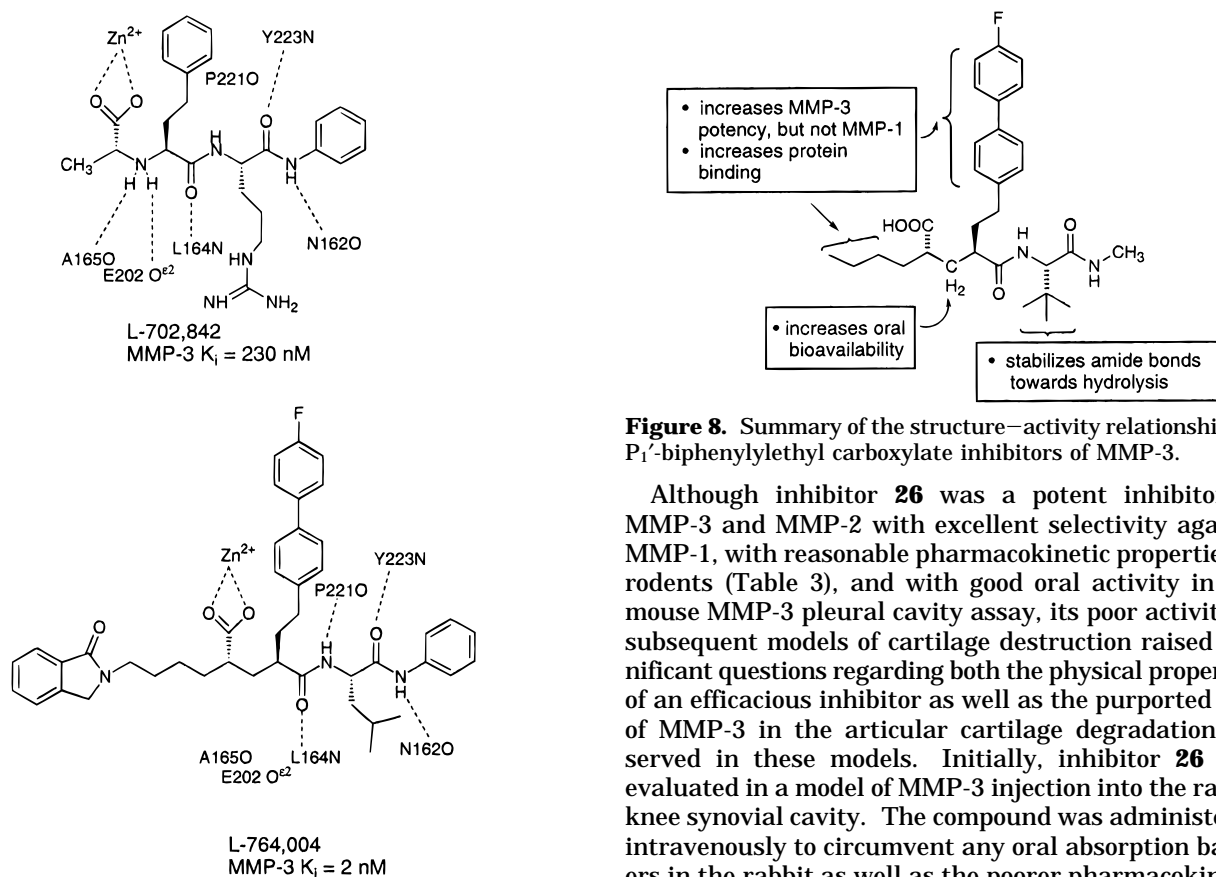


Figure 8. Summary of the structure–activity relationship for P_1' -biphenylethyl carboxylate inhibitors of MMP-3.

Figure 7. Comparison of the hydrogen-bonding interactions of two inhibitors complexed with the catalytic domain of human MMP-3 as determined by X-ray crystallography.

at P_1 and the biphenylethyl group at P_1' increased the intrinsic activity against MMP-3 and improved activity in the *in vivo* pleural cavity model. Changing the secondary amine to a methylene had a positive effect on oral bioavailability, as did incorporating a *tert*-butyl group at P_2' and a methyl group at P_3' . The combination of all these changes into compound **26** produced a potent inhibitor of MMP-3 that was well absorbed and showed good duration of action.

Although inhibitor **26** was a potent inhibitor of MMP-3 and MMP-2 with excellent selectivity against MMP-1, with reasonable pharmacokinetic properties in rodents (Table 3), and with good oral activity in the mouse MMP-3 pleural cavity assay, its poor activity in subsequent models of cartilage destruction raised significant questions regarding both the physical properties of an efficacious inhibitor as well as the purported role of MMP-3 in the articular cartilage degradation observed in these models. Initially, inhibitor **26** was evaluated in a model of MMP-3 injection into the rabbit knee synovial cavity. The compound was administered intravenously to circumvent any oral absorption barriers in the rabbit as well as the poorer pharmacokinetic profile seen in this species (Table 3) and was found to have an ED_{50} of 6 mg/kg iv in this assay, thus providing evidence that **26** was able to inhibit MMP-3 activity in the knee joint.

With respect to articular cartilage degradation, the MMP-3 injection model described above utilizes the appropriate substrate (endogenous cartilage) in a targeted tissue (the joint space) but employs exogenous enzyme instilled into the synovial cavity, not enzyme generated and released within the cartilage itself. The injection of the cytokine IL-1 β into the synovial cavity has been shown to cause the concomitant synthesis of

MMPs and cartilage destruction.^{58,77} Thus, cartilage proteoglycan release in the IL-1 β injection model represents the effects of endogenous enzyme on endogenous substrate. Inhibitor **26** is a potent inhibitor of rabbit MMP-3 ($K_i = 3.2$ nM) and was administered intravenously at 2 times the ED₅₀ obtained in the MMP-3 injection model (12 mg/kg iv) every 2 h to insure adequate plasma concentrations. This compound had no effect on proteoglycan release in this assay.

Whereas the two rabbit models of MMP-mediated joint destruction described above represent models of acute cartilage degradation, the articular cartilage degradation seen in arthritic diseases occurs over many years.^{78,79} Inhibitor **26** was evaluated in two rodent models of more chronic joint destruction: rat adjuvant-induced arthritis (AIA) and mouse collagen-induced arthritis (CIA).^{60–62} It had a more favorable pharmacokinetic profile in rodents than in the rabbit and one which supported long term oral administration (Table 3). In the rat AIA model, compound **26** (50 mg/kg po b.i.d.) was administered from day 0 and continued throughout the 21 days of the experiment. Total drug plasma levels of **26** were determined 5 h after the last dose on day 21 and found to be 49.8 ± 13.5 μ M. Compound **26** failed to demonstrate efficacy in any of the parameters examined in rat AIA (body weight, paw swelling, and thymus and spleen weights). In the mouse CIA model, **26** was administered at the same dose (50 mg/kg po b.i.d.) throughout the 29 days of the experiment. Total drug plasma levels of **26** were obtained at the end of the experiment (65.0 ± 44.5 μ M). Again, **26** failed to have a significant effect on the degree of incidence and severity of joint destruction evaluated in this model. A similar result in the CIA model was found with mice of the appropriate background lacking the MMP-3 gene (MMP-3 knock-out mice).⁸⁰

Several explanations for the lack of efficacy of a compound such as **26** in protecting cartilage from MMP-mediated destruction may be offered. Compound **26** was a potent inhibitor of mouse MMP-3 (mouse MMP-3 $K_i = 23$ nM), so species differences can be discounted. MMP-3 (and perhaps MMP-2) may not be involved in the models of cartilage degradation in which **26** was evaluated. The mouse CIA model was chosen because immunolocalization studies identified MMP-3 and MMP-3-generated cartilage cleavage products (VDIPEN) in areas of cartilage degradation in this model.^{81,82} However, the lack of efficacy seen with **26** and with the MMP-3 knock-out mice in the CIA model suggests that this enzyme is not important in this model. A potent MMP-1 and MMP-2 inhibitor was effective in limiting cartilage and bone destruction in the rat AIA model, suggesting that at least one of these two enzymes is operative in this model.⁸³ Rat enzyme data are not available for **26**, so the role of MMP-2 and MMP-3 in rat AIA cannot be convincingly assessed with this compound. Also, an inhibitor of MMP-1 and MMP-3 was effective *in vivo* in limiting collagen and proteoglycan loss from implanted femoral head cartilage in rats, suggesting that the MMP-1 component may be essential in protecting cartilage from degradation.⁸⁴

Tumor necrosis factor- α (TNF- α) is a cytokine that has been shown to be involved in many aspects of inflammation and tissue degradation.⁸⁵ A metalloproteinase that cleaves the precursor of TNF- α has been

identified as having several inhibitors.^{86–88} Compound **26** does not inhibit the release of TNF- α from monocytes nor the processing of proTNF- α ,⁸⁹ and thus, this compound would not be expected to have an effect on the involvement of TNF- α in the models described above.

As seen in Table 3, **26** had sufficient oral bioavailability, plasma half-life, and clearance rates in rodents to provide adequate coverage in these species following oral dosing. Indeed, the plasma levels obtained at the end of the AIA and CIA models suggest that more than adequate plasma levels of **26** were available to inhibit MMP-3. The high protein binding of **26** may have, in part, contributed to its lack of activity in the rat AIA and mouse CIA models, but even 99.9% protein binding would still have provided 50–65 nM concentrations of free drug available to inhibit active enzyme. The activity of **26** in the mouse pleural cavity and rabbit knee IL-1 β injection models suggests that **26** is still able to inhibit MMP-3-mediated processes in extravascular spaces such as the pleural cavity and knee joint. The pharmacokinetic parameters and protein binding of **26** are comparable to several efficacious nonsteroidal antiinflammatory drugs (NSAIDs), such as indomethacin, naproxen, and ibuprofen.⁹⁰ However, the high plasma levels of **26** do not guarantee sufficient cartilage penetration to reach the site of MMP-3 proteinase action. Despite a low molecular weight (MW = 512), the negative charge of **26** may limit its facile transport into the highly sulfated environment of articular cartilage resulting, perhaps, in relatively low cartilage concentrations of inhibitor. On the other hand, at least at a very high concentration (100 μ M), **26** was able to prevent IL-1 β - or retinoic acid-induced degradation of bovine articular cartilage.⁹¹ Neutral MMP inhibitors have been demonstrated to be active in preventing proteoglycan loss, albeit in different species and models of cartilage destruction: L-696,418, an *N*-carboxyalkyl dipeptide MMP-3 inhibitor, was efficacious (50%) in preventing the loss of proteoglycan in the IL-1 β injection model in the rabbit,⁵⁹ and CGS 27023A, a nonpeptide hydroxamic acid, prevented the loss of cartilage proteoglycan in a partial meniscectomy model in rabbits.⁹² In summary, the lack of activity of **26** in the rat AIA and mouse CIA models may be attributed to one or more contributing factors: noninvolvement of MMP-3 and MMP-2 in these models, the lack of inhibition of MMP-1 and/or TNF- α processing, high protein binding, poor cartilage penetration and insufficient potency, and free drug levels.

A definitive role for MMP involvement in cartilage degradation still remains elusive. Progress is being made to identify specific cleavage products by these metalloproteinases, and these are being correlated with both animal model results and clinical readouts. New metalloproteinases including membrane-type MMPs^{93,94} and cytokine processing^{86–88} with overlapping substrate specificities and inhibition profiles will make the process even more arduous. In order to help provide a more definitive role for MMP involvement in articular cartilage degradation, MMP inhibitors will not only need to be potent, perhaps selective, and orally bioavailable with appropriate pharmacokinetic parameters but may also require physical properties necessary for effective penetration of cartilage to inhibit their respective targets at the site of action.

Experimental Section

Chemistry. General Procedures. Proton NMR spectra were recorded on either a Varian XL-400 or Unity-500 NMR spectrometer. Chemical shifts are given on the δ scale. Spectra were measured at 20 °C for solutions in chloroform-*d* or methanol-*d*₄. Infrared spectra were obtained as thin films on sodium plates on Perkin-Elmer 295 or 1310 spectrometers. Mass spectra were determined on a LKB 9000 mass spectrometer. Analytical results for compounds followed by elemental symbols were +0.4% of calculated values unless otherwise indicated and were determined by Robertson-Microlit Laboratories, Inc., Madison, NJ. Thin layer chromatography was performed on precoated silica gel GHLF₂₅₄ plates (Analtech) or Kieselgel-60, and visualization was effected with UV light, iodine, or ceric sulfate (1%)–sulfuric acid (10% spray). Preparative flash and medium pressure column chromatographies were performed on silica gel 60 (EM Science; 40–63 μ m).

4(S)-Benzyl-3-[4-(4-iodophenyl)butyryl]oxazolidin-2-one (2). To a solution of (*p*-iodophenyl)butyric acid (5.0 g, 17.2 mmol) in 50 mL of dry THF at 0 °C was added triethylamine (3.12 mL, 22.4 mmol) followed by trimethylacetyl chloride (2.34 mL, 19.0 mmol), and the mixture was stirred for 1 h. In a separate flask, *n*-butyllithium (8.34 mL, 20.9 mmol, 2.5 M in hexanes) was added to a solution of (S)-(-)-4-benzyl-2-oxazolidinone (3.66 g, 20.7 mmol) in 25 mL of dry THF at -78 °C. This was stirred for 1 h and then added to the mixed anhydride via canula. This mixture was allowed to warm from 0 °C to room temperature with stirring overnight, then diluted with 1.0 N KHCO₃, and extracted with ethyl acetate. The combined organic layers were washed with water and brine, dried over magnesium sulfate, and concentrated *in vacuo*. The crude product was purified by medium pressure liquid chromatography (MPLC) on a 40 × 350 mm silica gel column eluting with 15% ethyl acetate/hexane to afford 7.21 g (97%) of the title compound as a white solid: ¹H-NMR (400 MHz, CDCl₃) δ 7.59 (d, 2H), 7.33–7.15 (m, 5H), 6.95 (d, 2H), 4.62 (m, 1H), 4.13 (d, 2H), 3.26 (dd, 1H), 2.93 (m, 2H), 2.72 (dd, 1H), 2.63 (t, 2H), 1.97 (m, 2H).

4(R)-[(4(S)-Benzyl-2-oxooxazolidin-3-yl)carbonyl]-6-(4-iodophenyl)hexanoic Acid tert-Butyl Ester (3). To a solution of titanium tetrachloride (1.46 mL, 13.3 mmol) in 25 mL of dry (distilled over calcium hydride) methylene chloride at 0 °C was added titanium isopropoxide (1.24 mL, 4.17 mmol). This mixture was stirred for 5 min at 0 °C; then diisopropylethylamine (3.05 mL, 17.5 mmol) was added. This was stirred for 15 min; then a solution of **2** (7.21 g, 16.7 mmol) in 25 mL of dry methylene chloride was added. This was stirred for 90 min at 0 °C; then *tert*-butyl acrylate (3.67 mL, 25.0 mmol) was added. The reaction mixture was stirred overnight at 0 °C, then allowed to warm to room temperature, and diluted with saturated ammonium chloride. The aqueous layer was extracted with methylene chloride; then the combined organic layers were washed with 2 N HCl, water, and brine, dried over sodium sulfate, and concentrated *in vacuo*. The crude product was purified by MPLC on a 40 × 350 mm silica gel column eluting with 10% ethyl acetate/hexane to afford 7.52 g (80%) of the title compound as a faint yellow oil: ¹H-NMR (400 MHz, CDCl₃) δ 7.55 (d, 2H), 7.32 (t, 2H), 7.27 (t, 1H), 7.18 (d, 2H), 6.91 (d, 2H), 4.52 (m, 1H), 4.11 (d, 2H), 3.82 (m, 1H), 3.29 (dd, 1H), 2.68 (dd, 1H), 2.56 (m, 2H), 2.24 (m, 2H), 2.02 (m, 2H), 1.89 (m, 1H), 1.73 (m, 1H), 1.42 (s, 9H).

2(R)-[2-(4-Iodophenyl)ethyl]pentanedioic Acid 5-tert-Butyl Ester (4). **3** (7.52 g, 13.4 mmol) was dissolved in a mixture of 3:1 THF/water (200 mL) and cooled to 0 °C. To this solution were added 30% hydrogen peroxide (6.09 mL, 53.7 mmol) and lithium hydroxide monohydrate (1.13 g, 26.8 mmol). This mixture was stirred at 0 °C for 3 h; then a solution of sodium sulfite (7.44 g, 59.1 mmol) in 40 mL of water was added along with 100 mL of 0.5 N sodium bicarbonate. This mixture was stirred for 2 h; then the THF was evaporated off on a Rotovap. This aqueous mixture was diluted with 2 N HCl to pH = 2 and then extracted with ethyl acetate. The combined organic layers were dried over sodium sulfate and concentrated *in vacuo*. The crude product was purified by MPLC on a 40 × 350 mm silica gel column eluting with 0.5% acetic acid in 20%

ethyl acetate/hexane to afford 4.18 g (75%) of the title compound as a faint yellow oil: ¹H-NMR (400 MHz, CDCl₃) δ 7.58 (d, 2H), 6.91 (d, 2H), 2.59 (m, 2H), 2.40 (m, 1H), 2.25 (m, 2H), 2.02–1.81 (m, 3H), 1.73 (m, 1H), 1.41 (s, 9H).

2(R)-[2-(4-Iodophenyl)ethyl]-4-butylpentanedioic Acid 5-tert-Butyl Ester (5). To a cooled solution of diisopropylamine (3.50 mL, 24.98 mmol) in 20 mL of dry THF at -78 °C was added *n*-butyllithium (10.39 mL, 2.5 M in hexanes). To this was added a solution of **4** (4.18 g, 9.99 mmol) in a mixture of 15 mL of dry THF and 10 mL of 1,3-dimethyl-3,4,5,6-tetrahydro-2(1*H*)-pyrimidinone (DMPU). The reaction mixture was stirred at -78 °C for 1 h and then warmed to 0 °C, and iodobutane (2.27 mL, 19.99 mmol) was added in one portion. This mixture was stirred overnight at 0 °C, warmed to room temperature, and then diluted with 2 N HCl. The aqueous layer was extracted with ethyl acetate. The combined organic layers were washed with 2 N HCl, water, and brine, dried over magnesium sulfate, and concentrated *in vacuo*. The resulting oil was purified by MPLC on a 40 × 350 mm silica gel column eluting with a gradient from 0 to 5% (5% acetic acid/MeOH)/methylene chloride to afford 4.08 g (86%) of the title compound as a mixture of diastereomers (ca. 2:1 *S,R*:*R,R*): ¹H-NMR (400 MHz, CDCl₃) δ 7.58 (d, 2H), 6.91 (d, 2H), 2.61 (m, 1H), 2.53 (m, 1H), 2.37 (m, 1H), 2.26 (m, 1H), 2.02–1.83 (m, 2H), 1.82–1.68 (m, 2H), 1.54 (m, 2H), 1.39 (s, 9H), 1.23 (m, 4H), 0.84 (t, 3H).

2(R)-[2-(4-Iodophenyl)ethyl]-4(S)-butylpentanedioic Acid 5-tert-Butyl Ester 1-[2-(Trimethylsilyl)ethyl] Ester (6). To a solution of **5** (1.48 g, 3.12 mmol) in 5 mL of THF were added (trimethylsilyl)ethanol (0.537 mL, 3.74 mmol), (dimethylamino)pyridine (76 mg, 0.62 mmol), and 1-[3-(dimethylamino)propyl]-3-ethylcarbodiimide hydrochloride (EDC) (1.20 g, 6.24 mmol). This mixture was stirred at room temperature overnight, then diluted with ethyl acetate, washed with saturated sodium bicarbonate and brine, dried over magnesium sulfate, and concentrated *in vacuo*. The resulting oil was purified by MPLC on a 40 × 350 mm silica gel column eluting with a gradient from 0 to 5% ethyl acetate/hexane. The fractions containing the lower *R_f* spot were separated and combined to afford 300 mg of the title compound as the pure *S,R* diastereomer, and the mixed fractions (725 mg) were combined and saved for further purification: ¹H-NMR (400 MHz, CDCl₃) δ 7.58 (d, 2H), 6.91 (d, 2H), 4.13 (t, 2H), 2.60–2.42 (m, 2H), 2.33 (m, 1H), 2.22 (m, 1H), 1.90 (m, 2H), 1.76 (m, 1H), 1.54 (m, 2H), 1.40 (s, 9H), 1.23 (m, 4H), 0.98 (t, 2H), 0.84 (t, 3H), 0.03 (s, 9H).

2(R)-[2-[4-(3-Thienyl)phenyl]ethyl]-4(S)-butylpentanedioic Acid 5-tert-Butyl Ester 1-[2-(Trimethylsilyl)ethyl] Ester (7). To a solution of **6** (300 mg, 0.52 mmol) in a mixture of 2 mL of toluene and 1 mL of ethanol were added thiophene-3-boronic acid (74 mg, 0.57 mmol), 2.0 M aqueous sodium carbonate (0.653 mL, 1.3 mmol), potassium bromide (68 mg, 0.57 mmol), and tetrakis(triphenylphosphine)palladium (30 mg, 0.03 mmol). This mixture was stirred at 95 °C with protection from light for 6 h and then allowed to cool to room temperature. The mixture was diluted with ethyl acetate, washed with 2 N NaOH and brine, dried over magnesium sulfate, and concentrated *in vacuo*. The resulting oil was purified by MPLC on a 21 × 300 mm silica gel column eluting with 4% ethyl acetate/hexane to afford 240 mg of the title compound as a brown oil: ¹H-NMR (400 MHz, CDCl₃) δ 7.49 (d, *J* = 8 Hz, 2H), 7.39 (d, *J* = 2 Hz, 1H), 7.35 (d, *J* = 2 Hz, 2H), 7.18 (d, *J* = 8 Hz, 2H), 4.16 (t, *J* = 7 Hz, 2H), 2.68–2.50 (m, 2H), 2.40 (m, 1H), 2.24 (m, 1H), 1.92 (m, 2H), 1.81 (m, 1H), 1.71 (m, 1H), 1.55 (m, 2H), 1.40 (s, 9H), 1.23 (m, 4H), 0.98 (t, 2H), 0.85 (t, *J* = 7 Hz, 3H), 0.03 (s, 9H).

2(R)-[2-[4-(3-Thienyl)phenyl]ethyl]-4(S)-butylpentanedioic Acid 5-tert-Butyl Ester (8). To a solution of **7** (240 mg, 0.45 mmol) in 1 mL of DMF was added 1.0 M tetrabutylammonium fluoride (0.68 mL, 0.68 mmol) in THF. This mixture was stirred at room temperature for 4 h, then diluted with ethyl acetate, washed with 2 N HCl and brine, dried over magnesium sulfate, and concentrated *in vacuo*. The resulting oil was purified by MPLC on a 21 × 130 mm silica gel column eluting with a gradient from 0 to 5% (5% acetic acid/methanol)/methylene chloride to afford 190 mg of the title

compound as a brown oil: $^1\text{H-NMR}$ (400 MHz, CDCl_3) δ 7.49 (d, $J = 8$ Hz, 2H), 7.39 (d, $J = 2$ Hz, 1H), 7.35 (d, $J = 2$ Hz, 2H), 7.18 (d, $J = 8$ Hz, 2H), 2.68–2.50 (m, 2H), 2.40 (m, 1H), 2.24 (m, 1H), 1.92 (m, 2H), 1.81 (m, 1H), 1.71 (m, 1H), 1.55 (m, 2H), 1.40 (s, 9H), 1.23 (m, 4H), 0.85 (t, $J = 7$ Hz, 3H).

2(R)-[2-[4-(3-Thienyl)phenyl]ethyl]-4(S)-butylpentanedioic Acid 1-((S)-tert-Butylglycine methylamide) 5-tert-Butyl Ester Amide (9). To a solution of **8** (190 mg, 0.45 mmol) in 2 mL of THF were added (S)-tert-butylglycine methylamide hydrochloride (90 mg, 0.5 mmol), *N*-methylmorpholine (0.060 mL, 0.54 mmol), 1-hydroxy-7-azabenzotriazole (74 mg, 0.54 mmol), and EDC (173 mg, 0.9 mmol). This mixture was stirred at room temperature overnight, then diluted with ethyl acetate, washed with saturated aqueous sodium bicarbonate and brine, dried over magnesium sulfate, and concentrated *in vacuo*. The crude product was purified by MPLC on a 21×300 mm silica gel column eluting with 20% ethyl acetate/methylene chloride to afford 135 mg of the title compound as a white solid: $^1\text{H-NMR}$ (400 MHz, CDCl_3) δ 7.49 (d, $J = 8$ Hz, 2H), 7.37 (d, $J = 2$ Hz, 1H), 7.34 (d, $J = 2$ Hz, 2H), 7.17 (d, $J = 8$ Hz, 2H), 6.23 (d, $J = 9$ Hz, 1H), 5.97 (br, 1H), 4.26 (d, $J = 8$ Hz, 1H), 2.80 (d, $J = 5$ Hz, 3H), 2.60 (m, 1H), 2.46 (m, 1H), 2.28 (m, 1H), 2.11 (m, 1H), 1.92 (m, 2H), 1.76 (m, 1H), 1.55 (m, 2H), 1.37 (s, 9H), 1.23 (m, 4H), 1.00 (s, 9H), 0.84 (t, $J = 7$ Hz, 3H).

2(R)-[2-[4-(3-Thienyl)phenyl]ethyl]-4(S)-butylpentanedioic Acid 1-((S)-tert-Butylglycine methylamide) Amide (58). To a solution of **9** (135 mg) in 2 mL of methylene chloride at 0°C were added 0.5 mL of trifluoroacetic acid (TFA) and 0.3 mL of anisole. This mixture was allowed to warm to room temperature with stirring overnight and then concentrated *in vacuo*. The resulting oil was purified by MPLC on a 21×130 mm silica gel column eluting with a gradient from 0 to 5% (5% acetic acid/methanol)/methylene chloride to afford 60 mg of the title compound as a white solid: m/z^+ = 501; $^1\text{H-NMR}$ (500 MHz, CDCl_3) δ 7.51 (br, 1H), 7.43 (d, $J = 8$ Hz, 2H), 7.36 (d, $J = 2$ Hz, 1H), 7.32 (m, 2H), 7.11 (d, $J = 8$ Hz, 2H), 6.52 (br, 1H), 4.44 (d, $J = 8$ Hz, 1H), 2.83 (d, $J = 4$ Hz, 3H), 2.61–2.52 (m, 2H), 2.49 (m, 2H), 2.08 (m, 1H), 1.92 (m, 1H), 1.79 (m, 2H), 1.52 (m, 2H), 1.30 (m, 4H), 1.05 (s, 9H), 0.88 (t, $J = 6$ Hz, 3H).

2(R)-[2-[4-(4-Fluorophenyl)phenyl]ethyl]-4(S)-butylpentanedioic Acid 1-((S)-tert-Butylglycine 4-pyridylamide) 5-tert-Butyl Ester Amide (12). To a solution of **11** (150 mg, 0.23 mmol) in a mixture of 2 mL of toluene and 1 mL of ethanol were added 4-fluorophenylboronic acid (35 mg, 0.25 mmol), 2.0 M aqueous sodium carbonate (0.283 mL, 0.57 mmol), and tetrakis(triphenylphosphine)palladium (13 mg, 0.01 mmol). This mixture was stirred at 95°C with protection from light for 6 h and then allowed to cool to room temperature. The mixture was diluted with ethyl acetate, washed with 2 N NaOH and brine, dried over magnesium sulfate, and concentrated *in vacuo*. The crude product was purified by MPLC on a 21×300 mm silica gel column eluting with a gradient from 0 to 5% (10% ammonium hydroxide/methanol)/methylene chloride to afford 80 mg of the title compound as a faint yellow solid: $^1\text{H-NMR}$ (400 MHz, CDCl_3) δ 8.92 (br, 1H), 8.37 (d, $J = 6$ Hz, 2H), 7.48 (dd, $J = 5$ Hz, 2H), 7.45 (d, $J = 6$ Hz, 2H), 7.42 (d, $J = 8$ Hz, 2H), 7.19 (d, $J = 8$ Hz, 2H), 7.08 (t, $J = 8$ Hz, 2H), 6.35 (br d, 1H), 4.42 (d, $J = 8$ Hz, 1H), 2.68 (m, 1H), 2.51 (m, 1H), 2.31 (m, 1H), 2.15 (m, 1H), 2.03–1.86 (m, 2H), 1.80 (m, 1H), 1.70 (m, 2H), 1.57 (m, 1H), 1.40 (m, 1H), 1.36 (s, 9H), 1.23 (m, 2H), 1.10 (s, 9H), 0.84 (t, $J = 6$ Hz, 3H).

2(R)-[2-[4-(4-Fluorophenyl)phenyl]ethyl]-4(S)-butylpentanedioic Acid 1-((S)-tert-Butylglycine 4-pyridylamide) Amide (24). To a solution of **12** (80 mg) in 1 mL of methylene chloride at 0°C was added 0.250 mL of trifluoroacetic acid (TFA). This mixture was allowed to warm to room temperature with stirring overnight and then concentrated *in vacuo*. The resulting oil was purified by MPLC on a 21×130 mm silica gel column eluting with a gradient from 0 to 15% (5% acetic acid/methanol)/methylene chloride to afford 29 mg of the title compound as a white solid: m/z^+ = 575; $^1\text{H-NMR}$ (400 MHz, CD_3OD) δ 8.38 (d, $J = 6$ Hz, 2H), 8.02 (d, $J = 8$ Hz, 1H), 7.69 (d, $J = 7$ Hz, 2H), 7.53 (dd, $J = 7$ Hz, 2H), 7.40 (d, $J = 8$ Hz, 2H), 7.19 (d, $J = 8$ Hz, 2H), 7.11 (t, $J = 9$ Hz, 2H),

4.44 (d, $J = 8$ Hz, 1H), 2.59 (t, $J = 8$ Hz, 2H), 2.37 (m, 1H), 1.98 (s, acetate), 1.93 (m, 1H), 1.83 (m, 1H), 1.58 (m, 3H), 1.31 (m, 4H), 1.08 (s, 9H), 0.90 (t, $J = 7$ Hz, 3H).

4-(4'-Fluorobiphenyl)-4-oxobutyric Acid (14). A 500 mL three-neck, round-bottom flask equipped with a mechanical stirrer, thermometer, and reflux condenser was charged with methylene chloride (125 mL). 4-Fluorobiphenyl (20.0 g, 0.116 mol) was added followed by succinic anhydride (11.6 g, 0.116 mol). The mixture was cooled in an ice bath, and aluminum chloride (30.9 g, 0.232 mol) was added in six equal portions at 10–15 min intervals. The ice bath was applied as needed to maintain the internal temperature near 15°C . After the last addition, the mixture was stirred at ambient temperature for 90 min and then at gentle reflux (37 – 39°C) for another 90 min. The reaction mixture was then cooled in an ice bath and poured into a stirred mixture of ice (300 g) and concentrated hydrochloric acid (40 mL). Additional water (500 mL) was added, and the resulting solid was filtered, washed with water, and dried by suction. The solid was recrystallized from hot acetic acid to afford 19.6 g (62%) of the title compound as a white crystalline solid: $^1\text{H-NMR}$ (400 MHz, CDCl_3) δ 8.02 (d, 1H), 7.62 (d, 1H), 7.58 (dd, 1H), 7.15 (t, 1H), 3.33 (t, 2H), 2.83 (t, 2H).

4-(4'-Fluorobiphenyl)butyric Acid (15). A mixture of **14** (19.6 g, 0.072 mol) in acetic acid (185 mL) and methanol (75 mL) was stirred overnight at 60°C in the presence of 20% palladium hydroxide-on-carbon (1.2 g) under an atmosphere of hydrogen gas. The catalyst was removed by filtration through Celite and the filter washed with acetic acid. The combined filtrate and washings were evaporated and coevaporated several times with toluene. The solid was taken up in warm acetic acid and the solution resubjected to the above hydrogenolysis conditions at room temperature for 24 h. The catalyst was removed as above, and the filtrate was evaporated and coevaporated several times with toluene to afford 18.3 g (98%) of the title compound as a white crystalline solid: $^1\text{H-NMR}$ (400 MHz, CDCl_3) δ 7.51 (dd, 1H), 7.44 (d, 1H), 7.23 (d, 1H), 7.09 (t, 1H), 2.70 (t, 2H), 2.49 (t, 2H), 1.99 (m, 2H).

4(S)-Benzyl-3-[4-(4'-fluorobiphenyl)butyryl]oxazolidin-2-one (16). To a solution of **15** (18.3 g, 0.071 mol) in methylene chloride (220 mL) was added *N,N*-dimethylformamide (362 μL). The solution was cooled in an ice bath, and oxalyl chloride (6.85 mL, 0.79 mol) was added dropwise with stirring over 10 min. The mixture was stirred at 0°C for 30 min and then at room temperature for 2 h. After evaporation, the resulting acid chloride was dried for 1 h *in vacuo*. To a solution of 4(S)-benzyl-2-oxazolidinone (11.4 g, 64.3 mmol) in dry THF (185 mL) at -78°C was added *n*-butyllithium (43.4 mL, 1.6 M in hexanes, 69.4 mmol) dropwise over 10 min while maintaining the temperature at or below -60°C . After 15 min, a solution of the acid chloride in THF (35 mL) was added rapidly, and the mixture was stirred for 30 min at -78°C . The cooling bath was then removed, and stirring was continued for 1 h. Saturated ammonium chloride (55 mL) was then added, and the reaction mixture was partitioned between ethyl acetate and water. The organic layer was washed with saturated brine solution, dried (Na_2SO_4), and evaporated. The product was purified by flash silica gel chromatography eluting with 15% ethyl acetate in hexane. The title compound was obtained as a white crystalline solid: yield 22.5 g (76%); $^1\text{H-NMR}$ (400 MHz, CDCl_3) δ 7.51 (dd, 1H), 7.47 (d, 1H), 7.18–7.33 (m, 6H), 7.09 (t, 1H), 4.63 (m, 1H), 4.16 (m, 2H), 3.28 (dd, 1H), 3.00 (m, 3H), 2.70–2.79 (m, 2H), 2.06 (m, 2H).

2(R)-[2-[4-(Phenylethynyl)phenyl]ethyl]-4(S)-butylpentanedioic Acid 5-tert-Butyl Ester 1-[2-(Trimethylsilyl)ethyl] Ester (17). To a solution of **6** (600 mg, 1.04 mmol) in a mixture of 2 mL of DMF and 2 mL of diisopropylamine were added phenylacetylene (160 mg, 1.57 mmol), copper(I) iodide (10 mg, 0.05 mmol), and bis(triphenylphosphine)palladium chloride (37 mg, 0.05 mmol). This mixture was stirred at room temperature overnight, then diluted with ethyl acetate, washed with 2 N NaOH and brine, dried over magnesium sulfate, and concentrated *in vacuo*. The crude product was purified by MPLC on a 21×300 mm silica gel column eluting with 2% ethyl acetate/hexanes to afford 550 mg of the title compound as a reddish oil: $^1\text{H-NMR}$ (400 MHz, CDCl_3) δ 7.50 (d, $J = 8$

Hz, 2H), 7.42 (d, $J = 8$ Hz, 2H), 7.32 (m, 3H), 7.13 (d, $J = 8$ Hz, 2H), 4.14 (t, 2H), 2.66–2.50 (m, 2H), 2.36 (m, 1H), 2.22 (m, 1H), 1.91 (m, 2H), 1.80 (m, 1H), 1.54 (m, 2H), 1.40 (s, 9H), 1.23 (m, 4H), 0.98 (t, $J = 7$ Hz, 2H), 0.85 (t, $J = 7$ Hz, 3H), 0.03 (s, 9H).

4(R)-(2-Iodoethyl)-2(S)-butylpentanedioic Acid 5-tert-Butyl Ester 1-[2-(Trimethylsilyl)ethyl] Ester (19). To a solution of toluene (25 mL) in a 50 mL round-bottom flask fitted with a stir bar and rubber septum were added imidazole (530 mg, 7.7 mmol), triphenylphosphine (2.9 g, 8.0 mmol), and iodine (1.63 g, 6.7 mmol). To this was added 4(R)-(2-hydroxyethyl)-2(S)-butylpentanedioic acid 5-tert-butyl ester 1-[2-(trimethylsilyl)ethyl] ester (2.0 g, 5.15 mmol). The reaction mixture was stirred between 40 and 50 °C under nitrogen until starting material was gone and then cooled to 0 °C, and saturated sodium bicarbonate (10 mL) was added with vigorous stirring. Enough iodine was added until the yellow color just persists; 10 mL of water was added, and the solution was extracted with 3 × 10 mL of methylene chloride. The organic layers were dried over MgSO₄, filtered, and concentrated under reduced pressure. Purification on silica gel of the crude product (2.5 g) (hexane/ethyl acetate, 98:2) gave two products, the more polar of which is the desired product (1.5 g, 58%); ¹H-NMR (400 MHz, CDCl₃) δ 4.17 (m, 2H), 3.19 (m, 2H), 3.08 (m, 2H), 2.5 (m, 1H), 2.25 (m, 1H), 2.15 (m, 1H), 2.04 (m, 1H), 1.95 (m, 1H), 1.55 (m, 2H), 1.44 (s, 9H), 1.25 (m, 4H), 1.00 (m, 2H), 0.89 (t, 2H, $J = 9$ Hz), 0.03 (s, 9H).

4(R)-(2-Biphenyl-3-ylethyl)-2(S)-butylpentanedioic Acid 5-tert-Butyl Ester 1-[2-(Trimethylsilyl)ethyl] Ester (20). To a solution of 19 (373 mg, 0.75 mmol) in a 5 mL round-bottom flask fitted with a Teflon stir bar and rubber septum were added 75 mg of zinc/copper couple (1.15 mmol), 1 mL of benzene, and 100 μL of dry dimethylformamide. The solution was stirred under nitrogen for 4 h at 70 °C and then cooled to 25 °C. To this was added 3-bromobiphenyl (116 mg), and the reaction mixture was sonicated with an ultrasonicator at 25–55 °C until the starting material was consumed (~2 h). The solution was filtered to remove the solids, and the solvent was removed under reduced pressure. Flash chromatography (97.5:2.5 hexane/ethyl acetate) gave 80 mg of product (30% yield); ¹H-NMR (400 MHz, CDCl₃) δ 7.57 (d, 2H, $J = 8$ Hz), 7.4 (m, 4H), 7.34 (m, 2H), 7.15 (d, 1H, $J = 8$ Hz), 4.17 (m, 4H), 2.65 (m, 1H), 2.60 (m, 1H), 2.45 (m, 1H), 2.25 (m, 1H), 1.95 (m, 1H), 1.85 (m, 1H), 1.55 (m, 2H), 1.38 (s, 9H), 1.25 (m, 4H), 1.00 (m, 2H), 0.84 (t, 2H, $J = 9$ Hz), 0.02 (s, 9H).

4(R)-[2-(4-Cyclohept-2,3-enylphenyl)ethyl]-2(S)-butylpentanedioic Acid 5-tert-Butyl Ester 1-[2-(Trimethylsilyl)ethyl] Ester (21). To a solution of 6 (250 mg, 0.435 mmol) in *N,N*-dimethylformamide (1 mL) were added tetrabutylammonium chloride (121 mg, 0.435 mmol), potassium acetate (128 mg, 1.30 mmol), palladium(II) acetate (2.5 mg, 0.011 mmol), and cycloheptene (254 μL, 2.18 mmol). The reaction mixture was stirred overnight at room temperature under a nitrogen atmosphere. It was then diluted with ethyl acetate, washed with water, dried (Na₂SO₄), and evaporated. The product was obtained pure by flash silica gel chromatography eluting with 5% diethyl ether in hexane: yield 150 mg (64%); ¹H-NMR (400 MHz, CD₃OD) δ 6.94–7.61 (m, 4H), 5.69–5.89 (m, 2H), 4.18 (m, 2H), 1.40 (s, 9H), 1.89 (t, 3H), 0.08 (s, 9H).

4(R)-[2-[4-(Trimethylstannanyl)phenyl]ethyl]-2(S)-butylpentanedioic Acid 5-tert-Butyl Ester 1-[2-(Trimethylsilyl)ethyl] Ester (22). To a solution of 6 (2.0 g, 3.48 mmol) in 20 mL of dioxane was added triphenylphosphine (18 mg, 0.07 mmol), lithium chloride (162 mg, 3.83 mmol), hexamethylditin (0.872 mL, 4.53 mmol), and tetrakis(triphenylphosphine)palladium (201 mg, 0.17 mmol). This mixture was stirred at 95 °C for 90 min, cooled to room temperature, then diluted with ethyl acetate, washed with 2 N NaOH and brine, dried over magnesium sulfate, and concentrated *in vacuo*. The crude product was purified by MPLC on a 40 × 350 mm silica gel column eluting with 2.5% ethyl acetate/hexanes to afford 1.42 g (67%) of the title compound as a colorless oil: ¹H-NMR (200 MHz, CDCl₃) δ 7.38 (d, $J = 8$ Hz, 2H), 7.13 (d, $J = 8$ Hz, 2H), 4.14 (t, 2H), 2.62–2.58 (m, 2H), 2.36 (m, 1H), 2.22 (m, 1H), 1.91 (m, 2H), 1.80 (m, 1H), 1.54

(m, 2H), 1.39 (s, 9H), 1.23 (m, 4H), 0.98 (t, $J = 7$ Hz, 2H), 0.83 (t, $J = 7$ Hz, 3H), 0.03 (s, 9H).

4(R)-[2-[4-[1-(tert-Butoxycarbonyl)-1H-indol-2-yl]phenyl]ethyl]-2(S)-butylpentanedioic Acid 5-tert-Butyl Ester 1-[2-(Trimethylsilyl)ethyl] Ester (23). To a mixture of 22 (300 mg, 0.49 mmol) in 2 mL of *N*-methyl-2-pyrrolidinone were added triphenylarsene (15 mg, 0.05 mmol), zinc chloride (1.47 mL, 1.47 mmol, 1.0 M diethyl ether solution), *N*-(tert-butoxycarbonyl)-2-iodoindole (235 mg, 0.74 mmol), and tris-(dibenzylideneacetone)dipalladium(0) (22 mg, 0.025 mmol). The mixture was stirred at 60 °C for 2 h, cooled to room temperature, diluted with ethyl acetate, washed with sodium bicarbonate and brine, dried over sodium sulfate, and concentrated *in vacuo*. The crude product was purified by silica gel chromatography eluting with 2.5% diethyl ether/hexanes to afford 116 mg of the title compound: ¹H-NMR (400 MHz, CDCl₃) δ 8.14 (d, 2H), 7.54 (d, 2H), 7.34–7.24 (m, 5H), 4.23 (t, 2H), 2.73–2.55 (m, 2H), 2.44 (m, 1H), 2.26 (m, 1H), 1.94 (m, 2H), 1.83 (m, 1H), 1.59 (m, 2H), 1.43 (s, 9H), 1.27 (m, 13H), 1.04 (t, 2H), 0.90 (t, 3H), 0.08 (s, 9H).

X-ray Crystallography. Recombinant human proSLN-247 was expressed in *Escherichia coli*, purified and activated to the mature form (residues 83–247) essentially as described for proSLN-255.⁹⁵ The expression level of proSLN-247 was similar to that of proSLN-255; however, upon lysis of the cells, more proSLN-247 was prone to degradation thus lowering the final yields of protein by 30–50%.

The inhibited complex was crystallized by hanging drop vapor diffusion. Protein solution contained 16.5 mg/mL SLN-255, 1.2 M excess L-764,004, 5.0 mM CaCl₂, 0.02% NaN₃, and 20 mM MES, pH = 6.5; the reservoir contained 10% PEG-6000, 5% saturated NH₄Cl, 0.02% NaN₃, and 0.1 M cacodylate, pH = 7.0. The crystals belong to the orthorhombic space group *C222*₁, with $a = 84.13$, $b = 85.35$, and $c = 55.25$ Å, and diffraction data extend to a resolution of 1.7 Å. Three-dimensional diffraction data were collected using an R-Axis IIC area detector and Cu Kα radiation from a Rigaku RU-200 rotating anode X-ray generator. Data were processed using the RAXIS package.⁹⁶

The structure was solved by difference Fourier methods using the protein portion of an isomorphous stromelysin complex with a different inhibitor, which had been solved by heavy-atom methods.³⁴ Electron density corresponding to the inhibitor was clearly visible in initial maps. Complete models were constructed by interactive model building⁹⁷ and refinement using X-PLOR including one cycle of simulated annealing.⁹⁸ A bulk solvent mask was included in the model, and in the later stages of refinement, the model was confirmed by 10% simulated-annealing omit maps.⁹⁹ The final model of the inhibited complex comprised residues 88–247, two Zn²⁺ ions, three Ca²⁺ ions, the bound inhibitor, and 143 ordered water molecules. Coordinates have been deposited in the Protein Data Bank,¹⁰⁰ with access code 1HFS, and crystallographic parameters are provided in the Supporting Information.

Biology. Mouse Pleural Cavity Assay. Mice (C57B1/6J; $n = 6–10$)¹⁰¹ were predosed orally with compound in a solution of 2% DMSO, 2% Cremophor, and 96% aqueous solution of 0.25% carboxymethylcellulose. After the dosing time, 0.2 mL of a 2.5 mg/mL solution of [³H]transferrin⁶³ was injected intrapleurally followed immediately by the injection of 0.3 mL of a 100 μg/mL buffered solution (20 mM Tris, pH = 7.5, 0.15 M NaCl, 10 mM CaCl₂, 0.02% NaN₃, 0.05% Brij) of trypsin-activated human MMP-3. After 30 min, the animals were sacrificed by carbon dioxide asphyxiation, and the pleural cavity was lavaged with 1 mL of cold buffer containing 20 mM phenanthroline to prevent continued transferrin degradation *in vitro*. The fluid was centrifuged (10 min at 3000 rpm); 50 μL of a 15% solution of trichloroacetic acid (TCA) or buffer was added to a 200 μL aliquot of the supernatant. TCA preparations were precipitated on ice for 30 min and then centrifuged (5 min at 10 000 rpm). The supernatant (125 μL) was then counted. A percent inhibition relative to controls was calculated according to the equation below, and the results are reported in Tables 1 and 2 under the heading PLCAV.

$$\% \text{ degradation} = \frac{\text{TCA-soluble counts}}{\text{total counts}}$$

$$\% \text{ inhibition} = [(\% \text{ degradation w/compd soln}) - (\% \text{ degradation in buffer})] / [(\% \text{ degradation w/o MMP-3 added}) - (\% \text{ degradation in buffer})]$$

Rabbit MMP-3 Injection Model. MMP-3-induced proteoglycan release was induced by injecting one stifle joint of female New Zealand white rabbits (Hazelton Farms, Denver, PA; ~3 months of age, $n = 4$) with a phosphate-buffered saline (PBS) solution (0.5 mL) containing 100 μg of trypsin-activated human recombinant MMP-3 and the other with PBS;⁵⁸ 1 h after MMP-3 injection, the rabbits were sacrificed by lethal injection (Socumb), and the joints were lavaged with PBS (2 \times 0.5 mL) and analyzed for sulfated proteoglycans by the described alcian blue method.^{56,57} Inhibitor **26** (in 2% DMSO, 2% Cremophor, 96% PBS) was administered intravenously 15 min prior to the injection of MMP-3, and a dose that effectively inhibited 50% of the proteoglycan release was obtained (ED₅₀ = 6 mg/kg iv).

Rabbit IL-1 β Injection Model. IL-1 β -induced proteoglycan release was induced by injecting one stifle joint of female New Zealand white rabbits (Hazelton Farms, Denver, PA; ~3 months of age, $n = 6$) with 0.5 mL of a PBS solution containing 327 ng of human recombinant IL-1 β and the other with the PBS;⁵⁸ 12 h later, the rabbits were sacrificed by lethal injection, and the joints were lavaged with 0.5 mL of PBS. Synovial lavage fluid was analyzed for sulfated proteoglycans by the alcian blue assay. Inhibitor **26** (12 mg/kg iv in 2% DMSO, 2% Cremophor, 96% PBS) was administered every 2 h from the time of the IL-1 β injection through the end of the experiment but failed to inhibit proteoglycan release compared to vehicle controls.

Rat Adjuvant-Induced Arthritis Model. Adjuvant-induced arthritis (AIA) was induced in female Lewis rats (~150 g, $n = 10$) by an intradermal injection of 0.5 mg of *Mycobacterium butyricum* in light mineral oil in the left hind foot pad. Body weights, radiographs, and foot volumes of the contralateral paw were determined on days 0, 14, and 21. Compound **26** (50 mg/kg po b.i.d.) and appropriate vehicles were started on day 0 and continued throughout the experiment. Blood (1 mL) was withdrawn by cardiac puncture under methoxyflurane anesthesia 5 h after the last dose to determine plasma levels of **26**. Rats were sacrificed by carbon dioxide inhalation on day 21. The thymus and spleen of all rats were removed and weighed. General necropsy noted that abdominal, peritoneal, and thoracic cavities were normal. Indomethacin (1 mg/kg/day po s.i.d.) was used as a positive control. Compound **26** failed to demonstrate efficacy in any of the parameters examined in rat AIA (body weight, paw swelling, and thymus and spleen weights). The compound level in plasma collected 5 h after the final dose was 25.5 \pm 6.9 $\mu\text{g}/\text{mL}$. Indomethacin inhibited the paw swelling by 80% in this experiment.

Mouse Collagen-Induced Arthritis Model. Collagen-induced arthritis was induced in 8–10 week old male B10.RIII mice (Jackson Laboratories) by an intradermal injection of a solution (100 μL) of lyophilized porcine type II collagen in complete Freund's adjuvant (CFA; H37 Ra. *Mycobacterium tuberculosis*; Difco) in the base of the tail. The mice were boosted by injecting human recombinant IL-1 β (327 ng in 100 μL of PBS) subcutaneously on days 13, 14, and 15 following type II collagen injection. Each paw was scored starting on day 16 using the following system: 0 = normal, 1 = one or two swollen toes, 2 = three or more toes swollen and/or extending into the carpus or tarsus, 3 = deformity of paw, 4 = ankylosis. Severity score was calculated by adding all of the scores of each paw and obtaining a mean for that group. Compound **26** (50 mg/kg po b.i.d., $n = 28$) was administered in a solution of 4% DMSO, 4% Cremophor, and 92% PBS, and indomethacin (1 mg/kg po s.i.d., $n = 10$), dexamethasone (1 mg/kg po s.i.d.), and cyclophosphamide (5 mg/kg po s.i.d., $n = 10$) were administered in an aqueous solution throughout the course of the experiment. Animals were sacrificed by carbon

dioxide inhalation on day 29, and blood was collected to determine plasma levels of **26**. A statistical analysis was conducted daily from day 16 to monitor the progress of the study. Incidence between treatment groups was compared using the Fisher's exact test. Total severity scores in the treatment group were compared to vehicle controls using a nonparametric Wilcoxon test. Statistical significance was determined by using a significance level of 0.05 throughout the analysis. Inhibitor **26** had no statistically significant effect on either the incidence or severity of collagen-induced arthritis in this study. Total compound plasma level was determined to be 33.3 \pm 22.8 $\mu\text{g}/\text{mL}$ at the end of the experiment.

Determination of Compound 26 Levels in Blood. At the time of euthanasia, blood was collected by venapuncture of the caudal vena cava. The blood was placed in heparinized tubes and spun and the resulting plasma used to determine blood levels. Compound **24** was used as an internal standard. A solution of **24** (1.5 μL in 50 μL of 1% BSA) was added to 0.15 mL of plasma; 2 mL of acetonitrile/TFA (100:0.01, v/v) was added while the samples were vortexed. After centrifugation, the supernatant was diluted with 10 mL of water containing 0.1% TFA. The samples were passed through a Waters C-18 Sep-Pak cartridge and washed with 5 mL of 0.1% TFA in water. The cartridge was then eluted with 4 mL of methanol containing 0.1% TFA, which was then dried under a stream of nitrogen. The extract was resuspended in 0.2 mL of HPLC mobile phase (*vide infra*) and put into autosample vials after sonication and centrifugation. The samples were injected onto a Zorbax Rx-C8 column (0.46 \times 25 cm) equilibrated with 10 mM 1-octanesulfate/acetonitrile/methanol/TFA (29:24:47:0.1, v/v) at a rate of 1.0 mL/min. The column eluate was monitored at 268 nm. Concentrations were determined by comparing the ratio of areas of **26** and **24** to a standard curve.

Supporting Information Available: Tables of crystallographic parameters (1 page). Ordering information can be found on any current masthead page.

References

- (1) Murphy, G.; Docherty, A. J. P. The Matrix Metalloproteinases and Their Inhibitors. *Am. J. Respir. Cell Mol. Biol.* **1992**, *7*, 120–125.
- (2) Docherty, A. J. P.; Murphy, G. The Tissue Metalloproteinase Family and the Inhibitor TIMP: a Study Using cDNAs and Recombinant Proteins. *Ann. Rheum. Dis.* **1990**, *49*, 469–479.
- (3) Murphy, G. J. P.; Murphy, G.; Reynolds, J. J. The Origin of Matrix Metalloproteinases and Their Familial Relationships. *FEBS Lett.* **1991**, *289*, 4–7.
- (4) Birkedal-Hansen, H.; Moore, W. G. I.; Bodden, M. K.; Windsor, L. J.; Birkedal-Hansen, B.; Decarlo, A.; Engler, J. A. Matrix Metalloproteinases: A Review. *Crit. Rev. Oral. Biol. Med.* **1993**, *4*, 197–250.
- (5) Docherty, A. J. P.; O'Connell, J.; Crabbe, T.; Angal, S.; Murphy, G. The Matrix Metalloproteinases and Their Natural Inhibitors: Prospects for Treating Degenerative Tissue Diseases. *Trends Biotechnol.* **1992**, *10*, 200–207.
- (6) Woessner, F. J. Matrix Metalloproteinases and Their Inhibitors in Connective Tissue Remodeling. *FASEB* **1991**, *5*, 2145–2154.
- (7) Welgus, H. G. Stromelysin Structure and Function. *Prog. Inflamm. Res. Ther.* **1991**, 61–67.
- (8) Girard, M. T.; Matsubara, M.; Kublin, C.; Tessier, M. J.; Cintron, C.; Fini, M. E. Stromal Fibroblasts Synthesize Collagenase and Stromelysin During Long-Term Tissue Remodeling. *J. Cell Sci.* **1993**, *104*, 1001–1011.
- (9) Roughley, P. J.; Nguyen, Q.; Mort, J. S.; Hughes, C. E.; Caterson, B. Proteolytic Degradation in Human Articular Cartilage: Its Relationship to Stromelysin. *Agents Actions Suppl.* **1993**, 149–159.
- (10) Dean, D. D.; Martel-Pelletier, J.; Pelletier, J.-P.; Howell, D. S.; Woessner, F. J. Evidence of Metalloproteinase and Metalloproteinase Inhibitor Imbalance. *J. Clin. Invest.* **1989**, *84*, 678–685.
- (11) Hasty, K. A.; Reife, R. A.; Kang, A. H.; Stuart, J. M. The Role of Stromelysin in the Cartilage Destruction that Accompanies Inflammatory Arthritis. *Arthritis Rheum.* **1990**, *33*, 388–397.
- (12) Okada, Y.; Shinmei, M.; Tanaka, O.; Naka, K.; Kimura, A.; Nakanishi, I.; Bayliss, M. T.; Iwata, K.; Nagase, H. Localization of Matrix Metalloproteinase-3 Stromelysin in Osteoarthritic Cartilage and Synovium. *Lab. Invest.* **1992**, *66*, 680–690.
- (13) Walakovits, L. A.; Moore, V. L.; Bhardwaj, N.; Gallick, G. S.; Lark, M. W. Detection of Stromelysin and Collagenase in Synovial Fluid from Patients with Rheumatoid Arthritis and Posttraumatic Knee Injury. *Arthritis Rheum.* **1992**, *35*, 35–42.

- (14) Ganu, V. S.; Hu, S.-I.; Melton, R.; Winter, C.; Goldberg, V. M.; Haqqi, T. M.; Malesud, C. J. Biochemical and Molecular Characterization of Stromelysin Synthesized by Human Osteoarthritic Chondrocytes Stimulated with Recombinant Human Interleukin-1. *Clin. Exp. Rheumatol.* **1994**, *12*, 489–496.
- (15) Emonard, H.; Grimaud, J.-A. Matrix Metalloproteinases: A Review. *Cell. Mol. Biol.* **1990**, *36*, 131–154.
- (16) Stetler-Stevenson, W. G.; Liotta, L. A.; Brown, P. D. Role of Type IV Collagenases in Human Breast Cancer. *Cancer Treat. Res.* **1992**, *61*, 21–41.
- (17) Johnson, W. H.; Roberts, N. A.; Borkakoti, N. Collagenase Inhibitors: Their Design and Potential Therapeutic Use. *J. Enzyme Inhib.* **1987**, *2*, 1–22.
- (18) Henderson, B.; Docherty, A. J. P.; Beeley, N. R. A. Design of Inhibitors of Articular Cartilage Destruction. *Drugs Future* **1990**, *15*, 495–508.
- (19) Johnson, W. H. Collagenase Inhibitors. *Drug News Perspect.* **1990**, *3*, 453–458.
- (20) Wahl, R. C.; Dunlap, R. P.; Morgan, B. A. Biochemistry and Inhibition of Collagenase and Stromelysin. *Annu. Rep. Med. Chem.* **1990**, *25*, 177–184.
- (21) Schwartz, M. A.; Van Wart, H. E. Synthetic Inhibitors of Bacterial and Mammalian Interstitial Collagenases. In *Progress in Medicinal Chemistry*; Ellis, G. P., Luscombe, D. K., Eds.; Elsevier Sci. Publ.: New York, 1992; Vol. 29, Chapter 8, pp 271–334.
- (22) Beeley, N. R. A.; Ansell, P. R. J.; Docherty, A. J. P. Inhibitors of Matrix Metalloproteinases (MMP's). *Curr. Opin. Ther. Patents* **1994**, *4*, 7–16.
- (23) Beckett, R. P.; Davidson, A. H.; Drummond, A. H.; Huxley, P.; Whittaker, M. Recent Advances in Matrix Metalloproteinase Inhibitor Research. *Drug Discovery Today* **1996**, *1*, 16–26.
- (24) (a) Morphy, J. R.; Nillican, T. A.; Porter, J. R. Matrix Metalloproteinase Inhibitors: Current Status. *Curr. Med. Chem.* **1995**, *2*, 743–762. (b) Hodgson, J. Remodeling MMPs. *Biotechnology* **1995**, *13*, 554–557.
- (25) Brown, P. A. *Osteoarthritis: Advances in Pathology, Diagnosis and Treatment*; Internal. Bus. Commun.: London, 1994; p 1.
- (26) Brown, P. D. Matrix Metalloproteinase Inhibitors: A Novel Class of Anticancer Agents. *Adv. Enzyme Regul.* **1995**, *35*, 293–301.
- (27) Haggmann, W. K.; Lark, M. W.; Becker, J. W. Inhibition of Matrix Metalloproteinases. *Annu. Rep. Med. Chem.* **1996**, *31*, 231–240.
- (28) Chapman, K. T.; Kopka, I. E.; Durette, P. L.; Esser, C. K.; Lanza, T. J.; Izquierdo-Martin, M.; Niedzwiecki, L.; Chang, B.; Harrison, R. K.; Kuo, D. W.; Lin, T.-Y.; Stein, R. L.; Haggmann, W. K. Inhibition of Matrix Metalloproteinases by N-Carboxyalkyl Peptides. *J. Med. Chem.* **1993**, *36*, 4293–4301.
- (29) Esser, C. K.; Kopka, I. E.; Durette, P. L.; Harrison, R. K.; Niedzwiecki, L. M.; Izquierdo-Martin, M.; Stein, R. L.; Haggmann, W. K. Inhibition of Matrix Metalloproteinases by N-Carboxyalkyl Peptides containing extended alkyl residues at P1'. *Bioorg. Med. Chem. Lett.* **1995**, *5*, 539–542.
- (30) Chapman, K. T.; Durette, P. L.; Caldwell, C. G.; Sperow, K. M.; Niedzwiecki, L. M.; Harrison, R. K.; Saphos, C.; Christen, A. J.; Olszewski, J. M.; Moore, V. L.; MacCoss, M.; Haggmann, W. K. Orally active inhibitors of stromelysin-1 (MMP-3). *Bioorg. Med. Chem. Lett.* **1996**, *6*, 803–806.
- (31) Gowravaram, M. R.; Tomczuk, B. E.; Johnson, J. S.; Delecki, D.; Cook, E. R.; Ghose, A. K.; Mathiowetz, A. M.; Spurlino, J. C.; Rubin, B.; Smith, D. L.; Pulvino, T.; Wahl, R. C. Inhibition of Matrix Metalloproteinases by Hydroxamates containing Heteroatom-based Modifications of the P1' group. *J. Med. Chem.* **1995**, *38*, 2570–2581.
- (32) Porter, J. R.; Beeley, N. R. A.; Boyce, B. A.; Mason, B.; Millican, A.; Millar, K.; Leonard, J.; Morphy, J. R.; O'Connell, J. P. Potent and Selective Inhibitors of Gelatinase-A: 1. Hydroxamic Acid Derivatives. *Bioorg. Med. Chem. Lett.* **1994**, *4*, 2741–2746.
- (33) Gooley, P. R.; O'Connell, J. F.; Marcy, A. I.; Cuca, G. C.; Salowe, S. P.; Bush, B. L.; Hermes, J. D.; Esser, C. K.; Haggmann, W. K.; Springer, J. P.; Johnson, B. A. The NMR Structure of the Inhibited Catalytic Domain of Human Stromelysin-1. *Nature: Struct. Biol.* **1994**, *1*, 111–118.
- (34) Becker, J. W.; Marcy, A. I.; Rokosz, L. L.; Axel, M. G.; Burbaum, J. J.; Fitzgerald, P. M. D.; Cameron, P. M.; Esser, C. K.; Haggmann, W. K.; Hermes, J. D.; Springer, J. P. Stromelysin-1: Three-Dimensional Structure of the Inhibited Catalytic Domain and of the C-Truncated Proenzyme. *Protein Sci.* **1995**, *4*, 1966–1976.
- (35) Lovejoy, B.; Cleasby, A.; Hassell, A. M.; Longley, K.; Luther, M. A.; Weigl, D.; McGeehan, G.; McElroy, A. B.; Drewry, D.; Lambert, M. H.; Jordan, S. R. Structure of the Catalytic Domain of Fibroblast Collagenase Complexed with an Inhibitor. *Science* **1994**, *263*, 375–377.
- (36) Borkakoti, N.; Winkler, F. K.; Williams, D. H.; D'Arcy, A.; Broadhurst, M. J.; Brown, P. A.; Johnson, W. H.; Murray, E. J. Structure of the Catalytic Domain of Human Fibroblast Collagenase Complexed with an Inhibitor. *Nature: Struct. Biol.* **1994**, *1*, 106–110.
- (37) Spurlino, J. C.; Smallwood, A. M.; Carlton, D. D.; Banks, T. M.; Vavra, K. J.; Johnson, J. S.; Cook, E. R.; Falvo, J.; Wahl, R. C.; Pulvino, T. A.; Wendoloski, J. J.; Smith, D. L. Structure of Mature Truncated Human Fibroblast Collagenase. *Proteins: Struct., Funct., Genet.* **1994**, *19*, 98–109.
- (38) Evans, D. A.; Bilodeau, M. T.; Somers, T. C.; Clardy, J.; Cherry, D.; Kato, Y. Enantioselective Michael Reactions - Diastereoselective Reactions of Chlorotitanium Enolates of Chiral N-Acyloxazolidinones with Representative Electrophilic Olefins. *J. Org. Chem.* **1991**, *56*, 5750–5752.
- (39) Miyaura, N.; Yanagi, T.; Suzuki, A. The Palladium-Catalyzed Cross-Coupling Reaction of Phenylboronic Acid with Haloarenes in the Presence of Bases. *Synth. Commun.* **1981**, *11*, 513–519.
- (40) Takayuki, O.; Miyaura, N.; Suzuki, A. Palladium-Catalyzed Cross-Coupling Reaction of Organoboron Compounds with Organic Triflates. *J. Org. Chem.* **1993**, *58*, 2201–2208.
- (41) Thompson, W.; Guadino, J. A. General Synthesis of 5-Arylnicotinates. *J. Org. Chem.* **1984**, *49*, 5237–5243.
- (42) Shieh, W.-C.; Carlson, J. A. A Simple Asymmetric Synthesis of 4-Arylphenylalanines via Palladium-Catalyzed Cross-Coupling Reaction of Arylboronic Acids with Tyrosine Triflate. *J. Org. Chem.* **1992**, *57*, 379–381.
- (43) Huth, A.; Beetz, I.; Schumann, I. Synthesis of Diaryl Compounds by Palladium-Catalyzed Reaction of Aromatic Triflates with Boronic Acids. *Tetrahedron* **1989**, *45*, 6679–6682.
- (44) Arcadi, A.; Cacchi, S.; Delmastro, M.; Marinella, F. 5-Vinyl-4-Pentynoic Acids Through the Palladium-Catalyzed Reaction of 4-Pentynoic Acid with Vinyl Triflates. *SYNLETT* **1991**, 409–411.
- (45) Arcadi, A.; Burini, A.; Cacchi, S.; Delmastro, M.; Marinelli, F.; Pietroni, B. R. Palladium-Catalyzed Reaction of Vinyl Triflates and Vinyl Aryl Halides with 4-Alkynoyl Acids - Regioselective and Stereoselective Synthesis of (E)- δ -Vinyl Aryl- γ -Methylene- γ -Butyrolactones. *J. Org. Chem.* **1992**, *57*, 976–982.
- (46) Cacchi, S.; Morera, E.; Ortar, G. Palladium-Catalyzed Reaction of Enol Triflates with 1-Alkynes. A New Route to Conjugated Enynes. *Synthesis* **1986**, 320–322.
- (47) Larock, R. C.; Gong, W. H.; Baker, B. E. Improved Procedures for the Palladium-Catalyzed Intermolecular Arylation of Cyclic Alkenes. *Tetrahedron Lett.* **1989**, *30*, 2603–2606.
- (48) Echavarren, A. M.; Stille, J. K. Palladium-Catalyzed Coupling of Aryl Triflates with Organostannanes. *J. Am. Chem. Soc.* **1987**, *109*, 5478–5486.
- (49) Ciattini, P. G.; Morera, E.; Ortar, G. An Efficient Synthesis of 3-Substituted Indoles by Palladium-Catalyzed Coupling Reaction of 3-Tributylstannylindoles with Organic Triflates and Halides. *Tetrahedron Lett.* **1994**, *35*, 2405–2408.
- (50) Farina, V.; Krishnan, B.; Marshall, D. R.; Roth, G. P. Palladium-Catalyzed Coupling of Arylstannanes with Organic Sulfonates: A Comprehensive Study. *J. Org. Chem.* **1993**, *58*, 5434–5444.
- (51) For a review of palladium-catalyzed reactions of organotin compounds, see: Mitchell, T. N. Palladium-Catalyzed Reactions of Organotin Compounds. *Synthesis* **1992**, 803–815.
- (52) Scott, W. J.; Stille, J. K. Palladium-Catalyzed Coupling of Vinyl Triflates with Organostannanes. Synthetic and Mechanistic Studies. *J. Am. Chem. Soc.* **1986**, *108*, 3033–3040.
- (53) Stork, G.; Isaacs, R. C. A. Cine Substitution in Vinylstannane Cross-Coupling Reactions. *J. Am. Chem. Soc.* **1990**, *112*, 7399–7400.
- (54) Dunn, M. J.; Jackson, R. F. W.; Pietruszka, J.; Wishart, N.; Ellis, D.; Wythes, M. J. Preparation of a Serine-Derived Organozinc Reagent in Tetrahydrofuran: Synthesis of Novel, Enantiomerically Pure Allenic, Acetylenic and Heteroaryl Amino Acids. *SYNLETT* **1993**, 499–500.
- (55) Lark, M. W.; Saphos, C. A.; Walakovits, L. A.; Moore, V. L. In Vivo Activity of Human Recombinant Tissue Inhibitor of Metalloproteinases (TIMP). Activity Against Human Stromelysin In Vitro and In the Rat Pleural Cavity. *Biochem. Pharmacol.* **1990**, *39*, 2041–2049.
- (56) Bonassar, L. J.; Jeffries, K. A.; Frank, E. H.; Moore, V. L.; Lark, M. W.; Bayne, E. K.; McDonnell, J.; Olszewski, J.; Haggmann, W.; Chapman, K.; Grodzinsky, A. J. In vivo effects of stromelysin on the composition and physical properties of rabbit articular cartilage in the presence and absence of a synthetic inhibitor. *Arthritis Rheum.* **1995**, *38*, 1678–1686.
- (57) Olszewski, J. M.; Moore, V. L.; McDonnell, J.; Williams, H.; Saphos, C. A.; Green, B. G.; Knight, W. B.; Chapman, K. T.; Haggmann, W. K.; Dorn, C. P.; Hale, J. J.; Mumford, R. A. Proteoglycan-degrading activity of human stromelysin-1 and leukocyte elastase in rabbit joints. Quantitation of proteoglycan and a stromelysin-induced HABR fragment of aggrecan in synovial fluid and cartilage. *Connect. Tissue Res.* **1996**, *33*, 291–299.
- (58) McDonnell, J.; Hoerrner, L. A.; Lark, M. W.; Harper, C.; Dey, T.; Lobner, J.; Eiermann, G.; Kazakis, D.; Singer, I. I.; Moore, V. L. Recombinant human interleukin-1 β -induced increase in levels of proteoglycans, stromelysin, and leukocytes in rabbit synovial fluid. *Arthritis Rheum.* **1992**, *35*, 799–805.
- (59) Moore, V. L. Unpublished results.

- (60) Brahn, E. Animal models of rheumatoid arthritis: clues to etiology and treatment. *Clin. Orthop. Related Res.* **1991**, *265*, 42–53.
- (61) Taugros, J. D.; Argentieri, D. C.; McReynolds, R. A. Adjuvant Arthritis. *Methods Enzymol.* **1988**, *162*, 339–355.
- (62) Wooley, P. H. Collagen-induced arthritis in the mouse. *Methods Enzymol.* **1988**, *162*, 361–373.
- (63) Okada, Y.; Nagase, H.; Harris, E. D. A Metalloproteinase from Human Rheumatoid Synovial Fibroblasts the Digests Connective Tissue Matrix Components. Purification and Characterization. *J. Biol. Chem.* **1986**, *261*, 14245–14255.
- (64) Sahoo, S. P.; Caldwell, C. G.; Chapman, K. T.; Durette, P. L.; Esser, C. K.; Kopka, I. E.; Polo, S. A.; Sperow, K. M.; Niedzwiecki, L. M.; Izquierdo-Martin, M.; Chang, B. C.; Harrison, R. K.; Stein, R. L.; MacCoss, M.; Hagmann, W. K. Inhibition of Matrix Metalloproteinases by N-Carboxyalkyl Dipeptides: Enhanced Potency and Selectivity with Substituted P1' Homophenylalanines. *Bioorg. Med. Chem. Lett.* **1995**, *5*, 2441–2446.
- (65) Brown, F. K.; Brown, P. J.; Bickett, D. M.; Chambers, C. L.; Davies, H. G.; Deaton, D. N.; Drewry, D.; Foley, M.; McElroy, A. B.; Gregson, M.; McGeehan, G. M.; Myers, P. L.; Norton, D.; Salovich, J. M.; Schoenen, F. J.; Ward, P. Matrix Metalloproteinases Inhibitors Containing a ((Carboxyalkyl)amino)zinc Ligand: Modification of the P1 and P2' Residues. *J. Med. Chem.* **1994**, *37*, 674–688.
- (66) Broadhurst, M. J.; Brown, P. A.; Johnson, W. H.; Lawton, G. Preparation of N-(N-Hydroxysuccinamoyl)amino Acid Derivatives as Matrix Metalloproteinase Inhibitors. Eur. Pat. Appl. EP-575844-A2, 1993.
- (67) Chapman, K. T.; Wales, J.; Sahoo, S. P.; Niedzwiecki, L. M.; Izquierdo-Martin, M.; Chang, B. C.; Harrison, R. K.; Stein, R. L.; Hagmann, W. K. Inhibition of Matrix Metalloproteinases by P1 substituted N-Carboxyalkyl Dipeptides. *Bioorg. Med. Chem. Lett.* **1996**, *6*, 329–332.
- (68) Campion, C.; Davidson, A. H.; Dickens, J. P.; Crimmin, M. J. Preparation of N-(4-(N-Hydroxyamino)succinyl)amino Acid Amides as Collagenase Inhibitors. PCT Pat. Appl. WO90/05719-A1, 1990.
- (69) Caldwell, C. G. Unpublished results. Aryl substitution at P₁ did enhance potency against stromelysin-1 *in vitro*, but these compounds showed low oral absorption, which led to lower activity in the pleural cavity assay.
- (70) Broadhurst, M. J.; Brown, P. A.; Johnson, W. H.; Lawton, G. Amino Acid Derivatives Eur. Pat. Appl. EP-497192-A2, 1992.
- (71) Goulet, J. L.; Kinneary, J. F.; Durette, P. L.; Stein, R. L.; Harrison, R. K.; Izquierdo-Martin, M.; Kuo, D. W.; Lin, T.-Y.; Hagmann, W. K. Inhibition of Stromelysin-1 (MMP-3) by Peptidyl Phosphinic Acids. *Bioorg. Med. Chem. Lett.* **1994**, *4*, 1221–1224.
- (72) Beckett, R. P.; Whittaker, M.; Miller, A.; Martin, F. M. Preparation of N-Acylated Amino Acid Amide Derivatives as Metalloproteinase Inhibitors. PCT Pat. Appl. WO95/19956-A1, 1995.
- (73) Garlardy, R. E. Galaridin-TM: Antiinflammatory Protease Inhibitor. *Drugs Future* **1993**, *18*, 1109–1111.
- (74) Beszant, B.; Bird, J.; Gaster, L. M.; Harper, G. P.; Hughes, I.; Karran, E. H.; Markwell, R. E. Synthesis of Novel Modified Dipeptide Inhibitors of Human Collagenase: β -Mercapto Carboxylic Acid Derivatives. *J. Med. Chem.* **1993**, *36*, 4030–4039.
- (75) Kopka, I. E. Unpublished results. The effect of modification of the P₂'-P₃' backbone and side chain residues of N-carboxyalkyl peptide inhibitors of matrix metalloproteinases. Presented at Inflammation Research Association 7th International Conference, Mt. Laurel Resort, PA, Aug. 25, 1994.
- (76) Owens, K.; Kreiter, P.; Durette, P. Unpublished results.
- (77) Henderson, B.; Thompson, R. C.; Hardingham, T.; Lewthwaite, J. Inhibition of interleukin-1-induced synovitis and articular cartilage proteoglycan loss in the rabbit knee by recombinant human interleukin-1 receptor antagonist. *Cytokine* **1991**, *3*, 246–249.
- (78) Lohmander, L. S.; Hoerner, L. A.; Lark, M. W. Metalloproteinases, Tissue Inhibitor, and Proteoglycan Fragments in Knee Synovial Fluid in Human Osteoarthritis. *Arthritis Rheum.* **1993**, *36*, 181–189.
- (79) Walakovits, L. A.; Moore, V. L.; Bhardwaj, N.; Gallick, G. S.; Lark, M. W. Detection of Stromelysin and Collagenase in Synovial Fluid from Patients with Rheumatoid Arthritis and Posttraumatic Knee Injury. *Arthritis Rheum.* **1992**, *35*, 35–42.
- (80) Mudgett, J. S.; Chartrain, N. A.; Christen, A.; McDonnell, J.; Shen, C. F.; Kawka, D. W.; Sargent, J.; Bayne, E. K.; Singer, I. I.; Trumbauer, M.; Hutchinson, N. I.; Visco, D. M. Collagen-induced arthritis in the stromelysin-1 (MMP-3) knock-out mouse. *Trans. Orthop. Res. Soc.* **1995**, *20* (1), 148–155.
- (81) Hasty, K. A.; Reife, R. A.; Kang, A. H.; Stuart, J. The role of stromelysin in the cartilage that accompanies inflammatory arthritis. *Arthritis Rheum.* **1990**, *33*, 388–397.
- (82) Singer, I. I.; Kawka, D. W.; Bayne, E. K.; Donatelli, S. A.; Weidner, J. R.; Williams, H. R.; Ayala, J. M.; Mumford, R. A.; Lark, M. W.; Glant, T. T.; Nabozny, G. H.; David, C. S. VDIPEN, a metalloproteinase-generated neopeptide, is induced and immunolocalized in articular cartilage during inflammatory arthritis. *J. Clin. Invest.* **1995**, *95*, 2178–2186.
- (83) Conway, J. G.; Wakefield, J. A.; Brown, R. H.; Marron, B. E.; Sekut, L.; Stimpson, S. A.; McElroy, A.; Menius, J. A.; Jeffreys, J. J.; Clark, R. L.; McGeehan, G. M.; Connolly, K. M. Inhibition of cartilage and bone destruction in adjuvant arthritis in the rat by a matrix metalloproteinase inhibitor. *J. Exp. Med.* **1995**, *182*, 449–457.
- (84) Karran, E. H.; Young, T. J.; Markwell, R. E.; Harper, G. P. *In vivo* model of cartilage degradation - effects of a matrix metalloproteinase inhibitor. *Ann. Rheum. Dis.* **1995**, *54*, 662–669.
- (85) Aggarwal, B. B.; Natarajan, K. Tumor necrosis factors: developments during the last decade. *Eur. Cytokine Network* **1996**, *7*, 93–124.
- (86) Mohler, K. M.; Sleath, P. R.; Fitzner, J. N.; Cerretti, P. N.; Alderson, M.; Kerwar, S. S.; Torrance, D. S.; Otten-Evans, C.; Greenstreet, T.; Weerawarna, K.; Kronheim, S. R.; Peterson, M.; Gerhart, G.; Kozlosky, C. J.; March, C. J.; Black, R. A. Protection against a lethal dose of endotoxin by an inhibitor of tumour necrosis factor processing. *Nature* **1995**, *370*, 218–220.
- (87) Gearing, A. J. H.; Beckett, P.; Christodoulou, M.; Churchill, M.; Clements, J.; Davidson, A. H.; Drummond, A. H.; Galloway, W. A.; Gilbert, R.; Gordon, J. L.; Leber, T. M.; Mangan, M.; Miller, K.; Nayee, P.; Owen, K.; Patel, S.; Thomas, W.; Wells, G.; Wood, L. M.; Wooley, K. Processing of tumour necrosis factor- α precursor by metalloproteinases. *Nature* **1995**, *370*, 555–557.
- (88) McGeehan, G. M.; Becherer, J. D.; Blast, R. C.; Boyer, C. M.; Champion, B.; Connolly, K. M.; Conway, J. G.; Furdon, P.; Karp, S.; Kidao, S.; McElroy, A. B.; Nichols, J.; Pryzwansky, K. M.; Schoenen, F.; Sekut, L.; Truesdale, A.; Verghese, M.; Warner, J.; Ways, J. P. Regulation of tumour necrosis factor- α processing by a metalloproteinase inhibitor. *Nature* **1994**, *370*, 558–561.
- (89) Kostura, M. Unpublished results.
- (90) Ritschel, W. A. *Handbook of Basic Pharmacokinetics*, 4th ed.; Drug Intelligence Publ.: Hamilton, IL, 1992; pp 531–549.
- (91) Bonassar, L. J.; Sandy, J. D.; Plass, A. K.; Hagmann, W. K.; Esser, C. K.; Lark, M. W.; Grodzinsky, A. J. Release of G1 domain and hyaluronan induced by IL-1 β and retinoic acid can be prevented by an MMP inhibitor. *Trans. Orthop. Res. Soc.* **1996**, *21* (1), 147–125.
- (92) O'Byrne, E. M.; Parker, D. T.; Roberts, E. D.; Goldberg, R. L.; MacPherson, L. J.; Blancuzzi, V.; Wilson, D.; Singh, H. N.; Ludewig, R.; Ganu, V. S. Oral Administration of a Matrix Metalloproteinase Inhibitor, CGS 27023A, Protects the Cartilage Proteoglycan Matrix in a Partial Meniscectomy Model of Osteoarthritis in Rabbits. *Inflamm. Res.* **1995**, *44* (Suppl. 2), S177–S178.
- (93) Büttner, F. H.; Chubinskaya, S.; Margerie, D.; Huch, K.; Flechtenmacher, J.; Cole, A. A.; Kuettner, K. E.; Bartnik, E. Membranetype matrix metalloproteinase (MT-MMP) is expressed in human articular cartilage. *Trans. Orthop. Res. Soc.* **1996**, *21* (1), 173–129.
- (94) Jawahar, S.; Birkhead, J. R.; Vasios, G. W. Membranetype matrix metalloproteinase is expressed in human chondrocytes. *Trans. Orthop. Res. Soc.* **1996**, *21* (1), 174–129.
- (95) Marcy, A. I.; Eiberger, L. L.; Harrison, R.; Chan, H.-K.; Hutchinson, N. H.; Hagmann, W. H.; Cameron, P. C.; Boulton, D. A.; Hermes, J. D., Human fibroblast stromelysin catalytic domain: Expression, purification, and characterization of a C-terminally truncated form. *Biochemistry* **1991**, *30*, 6476–6483.
- (96) *R-axis manual*; Rigaku Corp.: Tokyo, 1994.
- (97) Sack, J. S. CHAIN - A crystallographic modeling program. *J. Mol. Graph.* **1988**, *6*, 224–225.
- (98) Brünger, A. T. *X-PLOR: version 3.1, a system for X-ray crystallography and NMR*; Yale University Press: New Haven, London, 1992.
- (99) Hodel, A.; Kim, S.-H.; Brünger, A. T. Model bias in macromolecular crystal systems. *Acta Crystallogr. A* **1992**, *48*, 851–858.
- (100) Bernstein, F. C.; Koetzle, T. F.; Williams, G. J. B.; Meyer, E. F., Jr.; Brice, M. D.; Rodgers, J. R.; Kennard, O.; Shimanouchi, T.; Tasumi, M. The protein data bank: a computer-based archival file for macromolecular structures. *J. Mol. Biol.* **1977**, *112*, 535–542.
- (101) Female C57Bl/6 mice, 6–8 weeks of age, were purchased from Jackson Laboratories. All procedures with animals were approved by Merck Research Laboratories IACUC Committee.

JM960465T